



Skeletal morphology of the early Paleocene plesiadapiform *Torrejonia wilsoni* (Euarchonta, Palaechthonidae)

Stephen G.B. Chester ^{a, b, c, *}, Thomas E. Williamson ^d, Mary T. Silcox ^e, Jonathan I. Bloch ^f, Eric J. Sargis ^{g, h}

^a Department of Anthropology and Archaeology, Brooklyn College, City University of New York, 2900 Bedford Avenue, Brooklyn, NY 11210, USA

^b Department of Anthropology, Graduate Center, City University of New York, 365 Fifth Avenue, New York, NY 10016, USA

^c New York Consortium in Evolutionary Primatology, New York, NY, USA

^d New Mexico Museum of Natural History and Science, 1801 Mountain Road, NW, Albuquerque, NM 87104-1375, USA

^e Department of Anthropology, University of Toronto Scarborough, 1265 Military Trail, Scarborough, Ontario, M1C 1A4, Canada

^f Florida Museum of Natural History, University of Florida, 1659 Museum Road, Gainesville, FL 32611-7800, USA

^g Department of Anthropology, Yale University, P. O. Box 208277, New Haven, CT 06520, USA

^h Division of Vertebrate Paleontology, Peabody Museum of Natural History, New Haven, CT 06520, USA



ARTICLE INFO

Article history:

Received 26 August 2018

Accepted 5 December 2018

Available online 11 February 2019

Keywords:

Arboreality

Plesiadapiforms

Postcranium

Functional morphology

Positional behavior

ABSTRACT

Plesiadapiforms, like other Paleogene mammals, are known mostly from fossil teeth and jaw fragments. The several families of plesiadapiforms known from partial skeletons have all been reconstructed as arborealists, but differences in postcranial morphology among these taxa indicate a diversity of positional behaviors. Here we provide the first detailed descriptions and comparisons of a dentally associated partial skeleton (NMMNH P-54500) and of the most complete dentary with anterior teeth (NMMNH P-71598) pertaining to *Torrejonia wilsoni*, from the early Paleocene (late Torrejonian To3 interval zone) of the Nacimiento Formation, San Juan Basin, New Mexico, USA. NMMNH P-54500 is the oldest known partial skeleton of a plesiadapiform and the only known postcrania for the Palaechthonidae. This skeleton includes craniodental fragments with all permanent teeth fully erupted, and partial forelimbs and hind limbs with some epiphyses unfused, indicating that this individual was a nearly fully-grown subadult. Analysis of the forelimb suggests mobile shoulder and elbow joints, a habitually flexed forearm, and capacity for manual grasping. The hip joint allowed abduction and lateral rotation of the thigh and provides evidence for frequent orthograde postures on large diameter supports. Other aspects of the hind limb suggest a habitually flexed thigh and knee with no evidence for specialized leaping, and mobile ankle joints capable of high degrees of inversion and eversion. Although it is likely that some variability exists within the group, analysis of this skeleton suggests that palaechthonids are most like paromomyids among plesiadapiforms, but retain more plesiomorphic postcranial features than has been documented for the Paromomyidae. These observations are congruent with craniodental evidence supporting palaechthonids and paromomyids as closely related within the Paromomyoidea. The skeleton of *T. wilsoni* also demonstrates that many regions of the postcranium were already well adapted for arboreality within the first few million years of the diversification of placental mammals following the Cretaceous-Paleogene extinction event.

© 2018 Elsevier Ltd. All rights reserved.

1. Introduction

Most plesiadapiform taxa are known only from dental remains (Silcox et al., 2017). This is especially true of the geologically oldest

known plesiadapiforms from the early and middle Paleocene, so the substrate preference of nearly all of these taxa is unknown. Over the past decade, inferences regarding the positional behaviors of plesiadapiforms have mostly been limited to analyses of several dentally associated partial skeletons representing fairly derived species from four plesiadapiform families (Plesiadapidae, Carpolestidae, Paromomyidae, and Micromomyidae) from the late Paleocene and early Eocene (Bloch and Boyer, 2002, 2007; Bloch

* Corresponding author.

E-mail address: stephenchester@brooklyn.cuny.edu (S.G.B. Chester).

et al., 2007; Boyer and Bloch, 2008; Boyer, 2009). Results from analyses of postcranial skeletons suggest that while plesiadapiforms likely had a diversity of positional behaviors, they were all arboreal, used orthograde postures on vertical supports, and could grasp small diameter branches with their hands and feet (e.g., Szalay et al., 1975; Beard, 1991; Bloch and Boyer, 2007; Bloch et al., 2007; Boyer et al., 2013a, 2016). However, with the exception of several specimens of plesiadapids (e.g., Simpson, 1935) and isolated postcranial elements attributed to plesiadapiforms (e.g., Szalay and Drawhorn, 1980; Chester et al., 2015), the postcranial morphology of early and middle Paleocene plesiadapiforms has been unknown until the recent discovery of the first palaechthonid skeleton (Chester et al., 2017).

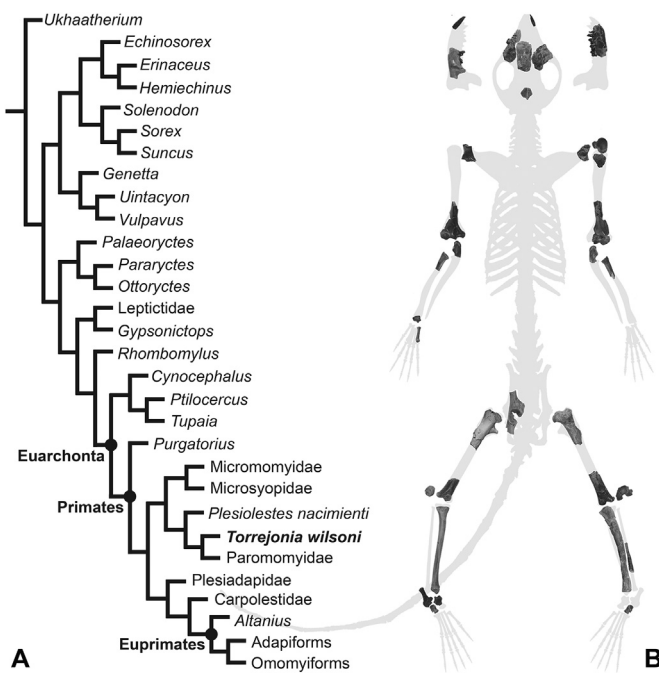
Palaechthonidae is a paraphyletic or polyphyletic group of plesiadapiforms with plesiomorphic dentitions from the Paleocene Torrejonian and Tiffanian North American Land Mammal Ages (NALMAs) of western North America (Silcox et al., 2017). Recent phylogenetic analyses support palaechthonids as most closely related to the Paromomyidae (Bloch et al., 2007; Silcox, 2008; Chester et al., 2017; Fig. 1A). Although palaechthonids are represented almost entirely by dental fossils, Wilson and Szalay (1972) reported one crushed partial cranium in their description of *Palaechthon nacimenti* (referred to here as *Plesiolestes nacimenti* following Gunnell, 1989; Silcox and Williamson, 2012). Kay and Cartmill (1977) provided a more detailed description of this partial cranium, which was the oldest and most primitive cranial fossil known for a plesiadapiform at the time, in order to try to better understand the “ecology of the ancestral primate stock” (Kay and

Cartmill, 1977:19). This description included the observations that *P. nacimenti* would have had small, widely separated and laterally oriented orbits, large infraorbital foramina likely associated with a well-innervated snout with many vibrissae, and a dentition that suggests a mostly insectivorous diet. Kay and Cartmill (1974, 1977) concluded that this species relied less heavily on vision and more on olfactory and tactile information, and suggested that it was adaptively similar to a hedgehog or some other terrestrial, foraging insectivore. Though postcrania of *P. nacimenti* are still unknown, initial assessment of the first postcrania of a palaechthonid suggested that this group was arboreal, like other known plesiadapiforms (Chester et al., 2017). Furthermore, some of the craniodental features previously cited as informative for terrestrial substrate preference occur in plesiadapiforms with postcranial adaptations for arboreality (e.g., small, laterally oriented orbits and large infraorbital foramina in the micromomyid *Dryomomys szalayi*; Bloch et al., 2007, 2016).

Here we provide the first detailed descriptions of the most complete dentary with anterior teeth (NMMNH P-71598) and the only known partial skeleton (NMMNH P-54500) of *Torrejonia wilsoni* and compare its skeletal morphology to that of other euarchoontan mammals (plesiadapiforms, euprimates, colugos, and treeshrews). NMMNH P-54500 is the oldest known partial skeleton of a plesiadapiform and the first known postcranial specimen representing the Palaechthonidae. The geologic age of this specimen and hypothesized fairly basal position of palaechthonids among plesiadapiforms (Bloch et al., 2007; Silcox, 2008; Ni et al., 2013, 2016; Chester et al., 2015, 2017) makes this partial skeleton important for understanding early euarchoontan and primate evolution (Fig. 1A).

The partial skeleton of *T. wilsoni* described here was collected at locality NMMNH L-6898 in the Ojo Encino Member of the Nacimiento Formation, San Juan Basin, New Mexico (Fig. 2). NMMNH L-6898 is within the Torrejonian (To3) NALMA *Mixodectes pungens* interval zone of Torrejon Wash (Williamson, 1996), which is the original ‘type locality’ for the Torrejonian NALMA (Wood et al., 1941). This locality dates to approximately 62.4 Ma (Leslie et al., 2018:Table 1, Fig. 3) based on its stratigraphic position within a normal polarity zone that is correlated with C27n and is bounded by upper and lower reversals dated at 62.221 Ma and 62.517 Ma, respectively (Ogg, 2012). This age estimate is supported by radiometric dating of detrital sanidines (62.48 ± 0.02 Ma) interpreted to be from a minimally reworked tephra layer from within this normal polarity zone (Leslie et al., 2018). See Chester et al. (2017) and Ksepka et al. (2017) for additional information on this locality and other fossil vertebrates collected at this site.

The recently discovered dentary described here (NMMNH P-71598) is from NMMNH locality L-9857, located near the head of Cañada Corrales, about 3.4 km northwest of locality L-6898. It is from strata that are closely correlative with those of L-6898. The locality occurs in pinkish siltstones located stratigraphically approximately midway between the ‘lower black’ and ‘upper black’ marker beds that delimit the Tj6 fossil zone (Leslie et al., 2018).



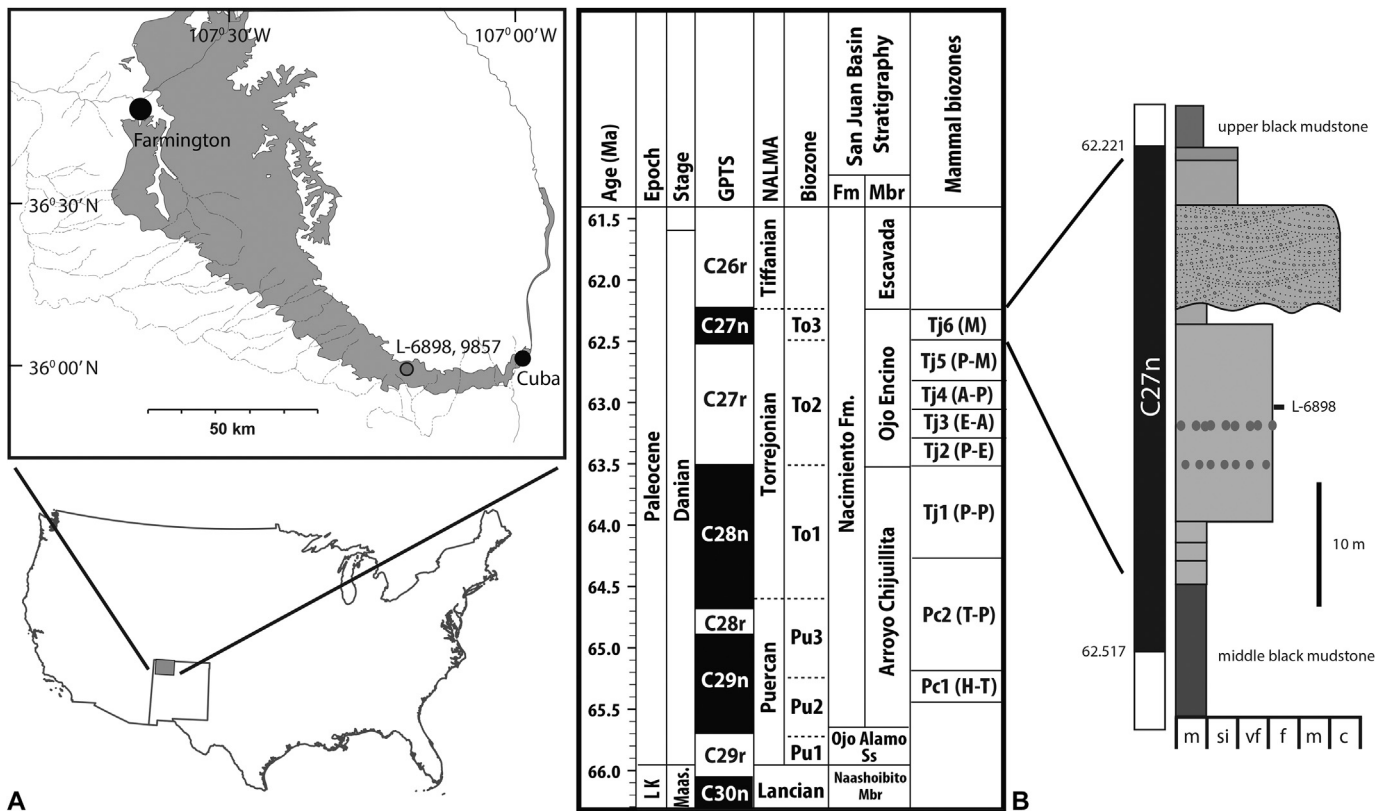


Figure 2. A) Map showing the location of fossil localities NMMNH L-6898 and 9857 relative to the outcrop belt of the Nacimiento Formation, San Juan Basin, New Mexico. B) Stratigraphic position of fossil locality NMMNH L-6898, relative to marker beds and paleomagnetic stratigraphy (Williamson, 1996) of a portion of the Nacimiento Formation, West Flank Torreon Wash and correlated to the Nacimiento Formation biostratigraphic zonation (Williamson, 1996), mammal biochronology (Paleocene NALMA and interval zones; Lofgren et al., 2004) and the geomagnetic polarity time scale (GPTS; after Ogg, 2012). The precise ages of the geomagnetic polarity reversals at the bottom and top of chron C27n are from Ogg (2012).

Museum of Paleontology, Ann Arbor, Michigan, USA; UNSM, University of Nebraska State Museum, Lincoln, Nebraska, USA; USNM, National Museum of Natural History, Smithsonian Institution, Washington D.C., USA.

2.2. Materials

There are no duplicated skeletal elements or tooth positions representing *T. wilsoni* (NMMNH P-54500) from NMMNH L-6898, which suggests that fossils of only one individual of this species were collected at this locality. However, it is important to note that this specimen was found mixed with partial skeletons of two other eutherian mammals, *M. pungens* (NMMNH P-54501) and *Acmeodon secans* (Cimolestidae; NMMNH P-54499). *Mixodectes pungens* is considerably larger than *T. wilsoni*, so skeletal elements were easily differentiated based on size. *Acmeodon secans* is similar in size to *T. wilsoni*, but many elements attributed to *T. wilsoni* closely resemble those of other dentally associated plesiadapiform skeletons. Postcranial elements tentatively attributed to *A. secans*, such as a partial axis, distal humerus, proximal radius, proximal femur, innominate, and calcaneus, are morphologically distinct from those attributed to *T. wilsoni* and other plesiadapiforms, and they are being analyzed in a separate study. Also like that of other dentally associated plesiadapiform skeletons (e.g., the micromomyid *Tinimomys graybulliensis*; [Chester and Bloch, 2013](#)), many long bones attributed to *T. wilsoni* have epiphyses that are not completely fused even though the adult dentition is fully erupted. We therefore interpret this individual of *T. wilsoni* as a nearly fully-grown subadult. The epiphyseal fusion present in postcranial elements attributed to *A. secans* (e.g., the proximal femur) indicates

that this individual was relatively more mature than *T. wilsoni* (Chester et al., 2017).

The partial skeleton of *T. wilsoni* (NMMNH P-54500) includes two cranial fragments, with associated left I₁, right dentary with P₂–M₂ and alveoli for I₁, I₂, C₁; left dentary with M₂–M₃ talonid; left maxilla with P⁴, M²–M³ and roots of P², P³, M¹; right isolated I¹, right maxilla with M¹–M³ (Silcox and Williamson, 2012:Fig. 8). Postcrania include the lateral portions of the left and right scapulae; portions of the left proximal and distal humerus and the right distal humerus; portions of the left and right proximal ulnae and the right distal ulnar epiphysis; portions of the left and right radii and the right distal radial epiphysis; the partial right innominate; portions of the left and right proximal femora and the left and right distal femora; nearly complete left and right tibiae; the right astragalar body; the right calcaneus; and the left and right cuboids. NMMNH P-71598 from NMMNH locality L-9857 is a left partial dentary with I₁–M₃ (C₁ broken, P₂ missing).

Additional fossil specimens examined include those of the archaic ungulate cf. *Protungulatum* (AMNH 118260, 118060), purgatoriid plesiadapiform cf. *Purgatorius* (UCMP 197509, 197517), micromomyid plesiadapiforms *D. szalayi* (UM 41870) and cf. *Tinimomys graybulliensis* (USNM 442277, 442280), paromomyid plesiadapiforms *Ignacius clarkforkensis* (UM 82606, 108210), cf. *Ignacius* (USNM 442235, 442240), and cf. *Phenacolemur simonsi* (USNM 442260), plesiadapid plesiadapiforms *Nannodectes gidleyi* (AMNH 17379) and *Plesiadapis cookei* (UM 87990), carpolestid plesiadapiform *Carpolestes simpsoni* (UM 101963), and adapiform euprimate *Notharctus tenebrosus* (AMNH 11474). Modern specimens examined include those of euprimates *Microcebus murinus* (USNM 83656, 83657) and *Galagooides demidoff* (AMNH 269904).

colugo *Cynocephalus volans* (AMNH 207001, ANSP 24797, USNM 15502), and treeshrews *Ptilocercus lowii* (MCZ 51736, USNM 488072) and *Tupaia gracilis* (FMNH 140928).

2.3. Methods

All measurements recorded for this study were taken (in mm) with Mitutoyo digital calipers under a Leica EZ4HD microscope. Maximum mesiodistal length and maximum buccolingual width dimensions of tooth crowns were recorded for NMMNH P-71598, and maximum length, width, and/or depth dimensions of postcranial elements (scapula, humerus, ulna, radius, innominate, femur, tibia, astragalus, calcaneus, cuboid, fifth metacarpal, and proximal phalanx) and/or specific bony features were recorded for NMMNH P-54500. Descriptions of all the measurements are provided in Tables 1 and 2.

Fossils of *T. wilsoni* (NMMNH P-54500, P-71598) were dusted with magnesium oxide to remove tonal contrasts and photographed using a Nikon D70 digital camera with a Nikon Micro-Nikkor 55 mm lens. Postcrania of other eutherian mammals were µCT scanned in a Scanco Medical µCT 35 machine housed in the Department of Internal Medicine at Yale University and a GE phoenix v|tome|x s240 housed at the American Museum of Natural History Microscopy and Imaging Facility Computed Tomography Laboratory. Renderings of 3D virtual models of specimens were generated in Avizo Lite 9.1 (FEI Visualization Sciences Group, Berlin).

3. Results

3.1. Description and comparisons

Cranium Two cranial fragments (Fig. 3) were found in association with the maxillary specimens of *T. wilsoni*. The larger of the two cranial fragments (Fig. 3A–C) preserves a portion of the right frontal bone, with a break located near what would have been the midline. On the rostral aspect of the frontal there is an indentation with a scalloped margin (Fig. 3A), which likely represents part of the sutural contact underlying the right nasal. The breadth of this indentation suggests that the frontonasal contact was broad, comprising much of the width of the frontal. The caudal part of the skull roof is missing, exposing what may be a portion of a natural endocast. If so, this would represent the rostral portion of the right cerebrum. The lateral edge of the frontal on the right exhibits a remnant of the temporal crest

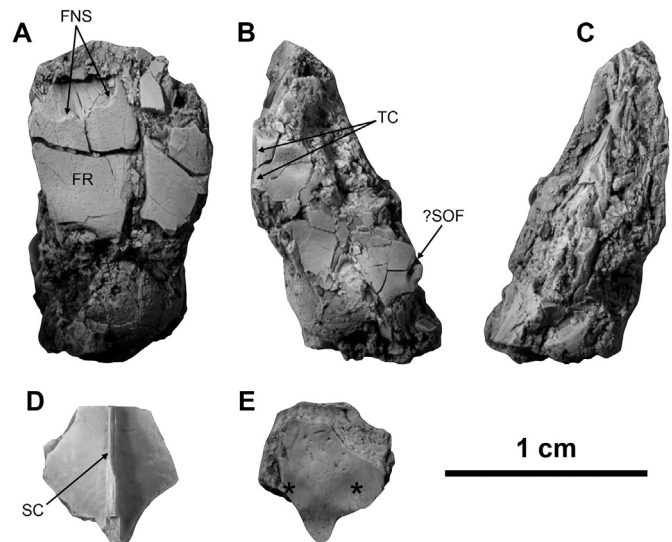


Figure 3. *Torrejonia wilsoni* (NMMNH P-54500) cranial fragments. A–C) Portion of the right frontal bone in dorsal (A), right lateral (B), and left lateral (C) views. D–E) Portion of fused parietals in dorsal (D) and ventral (E) views. Abbreviations: FNS = frontonasal suture; FR = frontal; SC = sagittal crest; ?SOF = ?sphenorbital fissure; TC = temporal crest; black asterisks = caudal colliculi.

(Fig. 3B). There is no evidence for a postorbital process. The temporal crest is damaged distally, so it is possible that a postorbital process was present but has broken away. However, in *Microsyops* (the only plesiadapiform that preserves a postorbital process in place; see Szalay, 1969:Fig. 16A), the process is located just caudal to the level of the frontonasal suture. This portion of the temporal crest is preserved in NMMNH P-54500, so the absence of a process in what is preserved suggests that the process was originally absent, at least in a position similar to that of *Microsyops*. In lateral view (Fig. 3B), there is a section of the lateral wall of the orbit located ventral to the temporal crest that exhibits numerous fractures and does not show any clear sutures, making it unclear whether there are any other cranial bones represented in the preserved fragment of the orbital wall. There is a single foramen located on the ventral aspect, near what would have likely been the distal extent of the orbit; this may be the sphenorbital fissure, but this is difficult to confirm in the absence of more contextual information.

The smaller cranial fragment (Fig. 3D–E) is likely a portion of fused parietals that bears a narrow sagittal crest on the dorsal surface (Fig. 3D). The ventral surface preserves most of a pair of shallow depressions placed on either side of the midline that formed the ceiling for what were likely the caudal (=inferior) colliculi (Fig. 3E). This indicates that a portion of the midbrain between the caudal aspect of the cerebrum and rostral aspect of the cerebellum was exposed, as in all plesiadapiforms in which the endocast is preserved (Gingerich and Gunnell, 2005; Silcox et al., 2009, 2010; Orliac et al., 2014), with the exception of a single specimen of *Microsyops annectans* in which the midbrain was covered by the venus sinus system (while another specimen of *Mi. annectans* has this portion of the midbrain exposed; Silcox et al., 2010).

The maxillae of *T. wilsoni* were illustrated previously by Silcox and Williamson (2012:Fig. 8) and Chester et al. (2017:Fig. 1B). Both are incomplete, yet preserve the root of the zygomatic processes, which extend from near the midline of M^2 to the mesial aspect of M^3 . Little of the palate remains, but the fragment of bone that is present medial to the roots of the anterior premolars on the left maxilla exhibits some evidence of rugosity to the bone, oriented rostrocaudally.

Table 1
Lower tooth crown measurements (in mm) for *Torrejonia wilsoni* (NMMNH P-71598).^a

Measurement	Value
I_1 length	~5.60
I_1 width	2.65
I_2 length	1.17
I_2 width	0.85
P_3 length	2.50
P_3 width	1.57
P_4 length	3.14
P_4 width	2.16
M_1 length	3.29
M_1 width	2.76
M_2 length	3.26
M_2 width	2.80
M_3 length	3.70
M_3 width	2.21

^a Length = maximum mesiodistal length; width = maximum buccolingual width.

Table 2Postcranial measurements (in mm) for *Torrejonia wilsoni* (NMMNH P-54500).

Measurement ^a	Value	Reference
Glenoid fossa length (SGL)	8.3	Sargis (2002a): Measurement 3
Glenoid fossa width (SGW)	4.7	Sargis (2002a): Measurement 4
Humeral head width (HHW)	6.0 (L)	Sargis (2002a): Measurement 6
Humeral head length (HHL)	6.8 (L)	Sargis (2002a): Measurement 7
Humeral trochlea width (HTW)	3.1	Sargis (2002a): Measurement 10
Humeral capitulum width (HCW)	5.7	Sargis (2002a): Measurement 11
Humeral trochlea length (HTL)	2.5	Sargis (2002a): Measurement 12
Humeral capitulum width (HCL)	3.6	Sargis (2002a): Measurement 13
Humeral trochlea depth (HTD)	4.0	Sargis (2002a): Measurement 14
Humeral distal articular surface width (HDASW)	8.8	Sargis (2002a): Measurement 15
Humeral distal end width (HDEW)	13.6	Sargis (2002a): Measurement 16
Humeral medial epicondyle width	4.8	Boyer et al. (2010): Figure 5A
Ulnar olecranon process length (UOPL)	5.7	Sargis (2002a): Measurement 19
Ulnar trochlear notch width (UTNW)	3.2 (L)	Sargis (2002a): Measurement 20
Ulnar styloid process length (USPL)	1.6	Sargis (2002a): Measurement 23
Radial neck length (RNL)	6.2	Sargis (2002a): Measurement 27
Radial head width (RHW)	5.0	Sargis (2002a): Measurement 28
Radial head rim length (RHRL)	1.5	Sargis (2002a): Measurement 29
Radial styloid process length (RSPL)	0.9	Sargis (2002a): Measurement 30
Radial distal end width (RDEW)	4.9	Sargis (2002a): Measurement 31
Radial distal end length (RDEL)	4.0	Sargis (2002a): Measurement 32
Radial head length (RHL)	3.8	Sargis (2002a): Measurement 33
MC5 maximum proximodistal length	8.8	Boyer et al. (2013a): Figure 6
Acetabulum length (IAL)	8.5	Sargis (2002c): Measurement 4
Acetabulum width (IAW)	7.6	Sargis (2002c): Measurement 5
Femoral patellar groove width (FPGW)	4.4 (L)	Sargis (2002c): Measurement 18
Femoral distal end width (FDEW)	9.7 (L)	Sargis (2002c): Measurement 19
Femoral medial condyle depth (FMCD)	6.8 (L)	Sargis (2002c): Measurement 20
Femoral lateral condyle depth (FLCD)	6.7 (L)	Sargis (2002c): Measurement 21
Femoral medial condyle width (FMCW)	3.4 (L)	Sargis (2002c): Measurement 22
Femoral lateral condyle width (FLCW)	3.5 (L)	Sargis (2002c): Measurement 23
Femoral medial condyle length (FMCL)	4.3 (L)	Sargis (2002c): Measurement 24
Femoral lateral condyle length (FLCL)	4.4 (L)	Sargis (2002c): Measurement 25
Femoral intercondylar notch width (FICNW)	2.1 (L)	Sargis (2002c): Measurement 26
Tibial distal end width (TDEW)	5.0	Sargis (2002c): Measurement 36
Tibial medial malleolus length (TMML)	1.2	Sargis (2002c): Measurement 37
Tibial medial malleolus width (TMMW)	2.1	Sargis (2002c): Measurement 38
Tibial distal articular surface (lateral astragalar facet) width (TDASW)	2.8	Sargis (2002c): Measurement 39
Tibial distal articular surface (lateral astragalar facet) length (TDASL)	4.8	Sargis (2002c): Measurement 40
Astragalar fibular facet dorsoplantar depth	2.9	Chester et al. (2015): Astragalar measurement 4
Astragalar fibular facet proximodistal length	4.3	Chester et al. (2015): Astragalar measurement 5
Astragalar flexor fibularis groove mediolateral width	2.5	Chester et al. (2015): Astragalar measurement 12
Astragalar lateral tibial facet maximum mediolateral width	2.8	Chester et al. (2015): Astragalar measurement 7
Astragalar ectal facet proximodistal length	3.4	Chester et al. (2015): Astragalar measurement 10
Astragalar ectal facet mediolateral width	2.4	Chester et al. (2015): Astragalar measurement 11
Calcaneal maximum proximodistal length	11.7	Chester et al. (2015): Calcaneal measurement 1
Calcaneal tuber + ectal facet proximodistal length	7.6	Chester et al. (2015): Calcaneal measurement 2
Calcaneal ectal facet proximodistal length	3.5	Chester et al. (2015): Calcaneal measurement 7
Calcaneal cuboid facet dorsoplantar depth	2.7	Chester et al. (2015): Figure S2
Calcaneal cuboid facet mediolateral width	3.6	Chester et al. (2015): Figure S2
Cuboid maximum proximodistal length	5.0	This study: Figure 13, ML
Cuboid distal facet dorsoplantar depth	2.6	This study: Figure 13, DD
Cuboid distal facet mediolateral width	3.0	This study: Figure 13, DW
Proximal phalanx maximum proximodistal length	10.8	Gebo et al. (2015): Figure 1

^a All measurements provided are either standard postcranial measurements or functionally relevant to this study. They were taken from the right side of the skeleton unless otherwise indicated (L = left).

Dentition and dentary The dentition associated with the partial skeleton of *T. wilsoni* (NMMNH P-54500) was described previously by Silcox and Williamson (2012). A more recently discovered and more complete left dentary (NMMNH P-71598; Fig. 4) preserves the most complete lower anterior teeth (I_1 , I_2 , C_1) known for *T. wilsoni* and confirms the attribution of an isolated partial I_1 to NMMNH P-54500 by Silcox and Williamson (2012). Examination of NMMNH P-71598 also confirms the previous hypothesis that the lower dental formula of *T. wilsoni* is 2.1.3.3 with no evidence of I_3 or P_1 present (Silcox and Williamson, 2012).

The lower central incisor crown of NMMNH P-71598 is mostly complete, but is broken slightly at the midpoint of the apical-basal margin and the very apex is missing (Fig. 4). The I_1 of *T. wilsoni* is

procumbent, and relatively short and broad. Like the I_1 of NMMNH-54500, the occlusal surface of the crown of NMMNH P-71598 is quite flat, being bounded by ridges laterally and medially, but with no margoconid present. The occlusal surface bears a faint central ridge that runs from the apex to the base. The I_1 has a somewhat lanceolate shape, expanding in length (sensu Bloch and Gingerich, 1998:Fig. 1) from the base, but narrowing again near the tip. Among palaechthonids, the overall shape of I_1 is most similar to that of the plesiolestine *Plesiolestes problematicus* and differs from the more laterally compressed, less lanceolate condition of the palaechthonine *Palenochtha minor* (see Gunnell, 1989:Fig. 5a,b). The I_1 of *T. wilsoni* is also similar in shape to the distinctively lanceolate I_1 of North American microsyopids (see Silcox et al., 2017:Fig. 3).

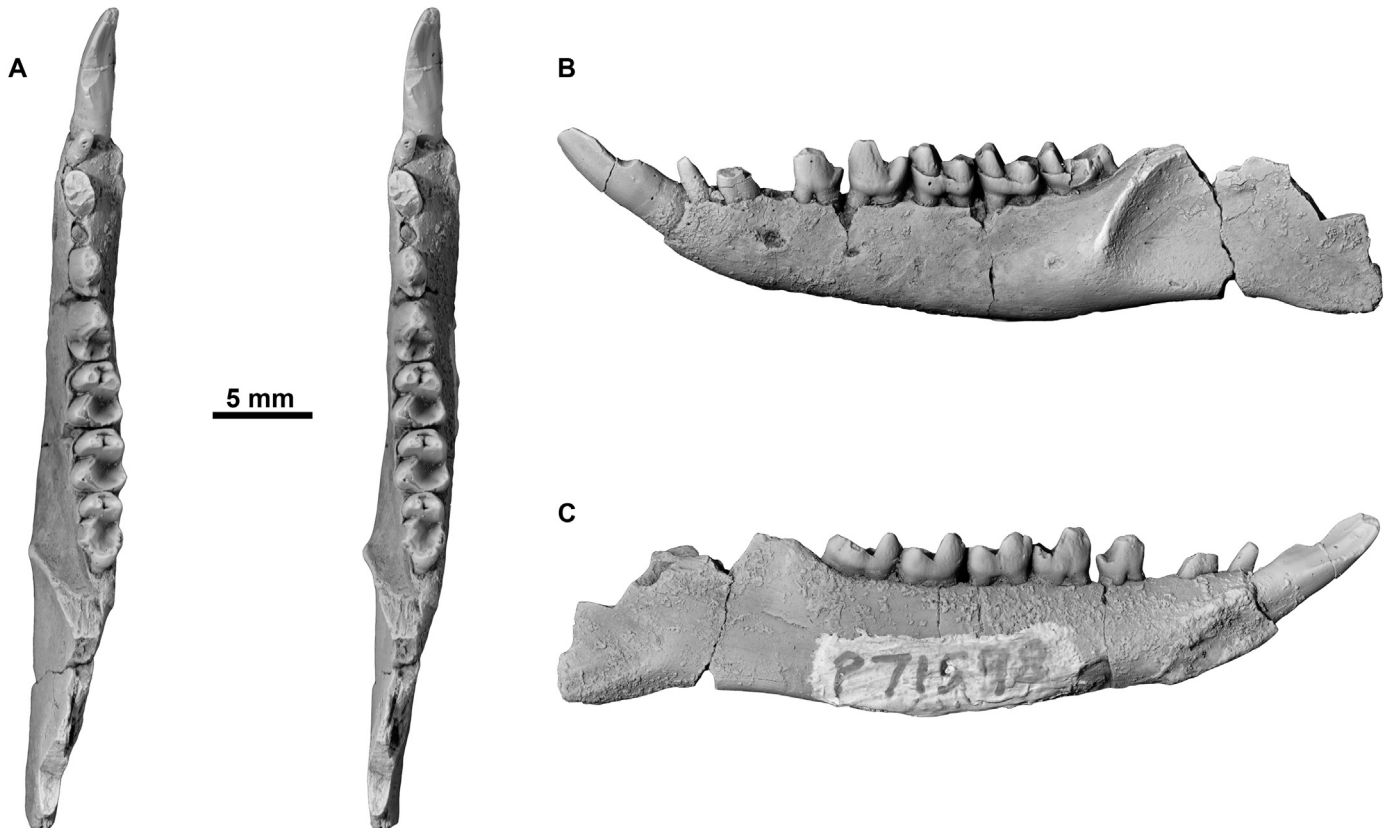


Figure 4. *Torrejonia wilsoni* (NMMNH P-71598) left partial dentary I_1 – M_3 (C_1 broken, P_2 missing) in occlusal (A, stereo pair), buccal (B), and lingual (C) views.

NMMNH P-71598 also shows that the I_1 in *T. wilsoni* is oriented slightly more medially than that tooth in *P. problematicus*, being similar in this way to microsyopids. The similarity in I_1 shape between plesiolestines and microsyopids has been suggested to be evidence of their close relationship (Bown and Gingerich, 1973; Gunnell, 1989), although this link has not been recovered in broadly sampled phylogenetic analyses including both groups (e.g., Bloch et al., 2007; Silcox, 2008; Chester et al., 2017).

NMMNH P-71598 is the only known specimen of *T. wilsoni* that preserves the crown of I_2 . It is conical, very simple, and oriented anteriorly about 60° relative to the tooth row (Fig. 4B). It is approximately the same size as the crown of P_2 in NMMNH P-54500, and the teeth in those two positions are the smallest in the lower tooth row. The crown of the canine is broken, but enough of the tooth is preserved to see that it was oriented slightly anteriorly and was mediolaterally narrower than mesiodistally long. Based on the size of its alveolus and root, the canine crown would have been considerably larger than that of P_2 (Fig. 4A; Silcox and Williamson, 2012:Fig. 8l), which supports *T. wilsoni* as a member of the sub-family Plesiolestinae (Gunnell, 1989). All remaining lower premolar and molar tooth positions have already been thoroughly described for *T. wilsoni* (see Silcox and Williamson, 2012), and these tooth positions in NMMNH P-71598 fall within previously documented patterns of variation for this taxon (Table 1).

The discovery of NMMNH P-54500 and P-71598 allow for the description of several undocumented aspects of the dentary of *T. wilsoni*. They preserve the symphysis, which terminates on the medial surface below and just anterior to P_3 (Fig. 4C; Silcox and Williamson, 2012:Fig. 8m). These specimens also preserve several mental foramina located approximately along the dorsoventral midline of the lateral side of the dentary. The largest mental

foramen in both specimens is positioned below P_2 (Fig. 4B; Silcox and Williamson, 2012:Fig. 8l). The second largest mental foramen is positioned below the midpoint of P_4 in NMMNH P-54500 (Silcox and Williamson, 2012:Fig. 8l) and below the anterior root of P_4 in NMMNH P-71598 (Fig. 4B). NMMNH P-54500 has two additional smaller foramina. The first is below the position for C_1 and the second is below the posterior root of P_4 (Silcox and Williamson, 2012:Fig. 8l). Both specimens also preserve the anterior margin of the masseteric fossa, which is just posterior to the position of M_3 (Fig. 4B; Silcox and Williamson, 2012:Fig. 8o).

Vertebrae and sternebrae The vertebrae and sternebrae recovered at locality NMMNH L-6898 that are within the expected size range for *T. wilsoni* and *A. secans* are rather fragmentary and none is attributed to the partial skeleton of *T. wilsoni* at this time. These elements include what are interpreted as four partial sternebrae, one partial axis, three additional partial cervical vertebrae, five thoracic vertebral bodies, six lower thoracic and/or upper lumbar vertebral bodies, and five partial caudal vertebrae. The axis preserves an odontoid process that is straight and oriented cranially, whereas the odontoid process is angled more dorsally in plesiadapiforms and other euarchontans such as treeshrews (see Sargis, 2001:Fig. 2). Therefore, this partial axis likely represents *A. secans*. Although some of the other fragmentary vertebrae and sternebrae may belong to *T. wilsoni*, we cannot currently attribute them to this partial skeleton with any confidence.

Scapula All that remains of both scapulae of *T. wilsoni* are the most lateral portions of these bones, including the base of the coracoid, the base of the most lateral aspect of the scapular spine, and a fairly complete glenoid fossa (Fig. 5). The right scapula is less abraded and compressed, and preserves a more complete glenoid fossa, which is concave and wider inferiorly than superiorly. The pear-shaped

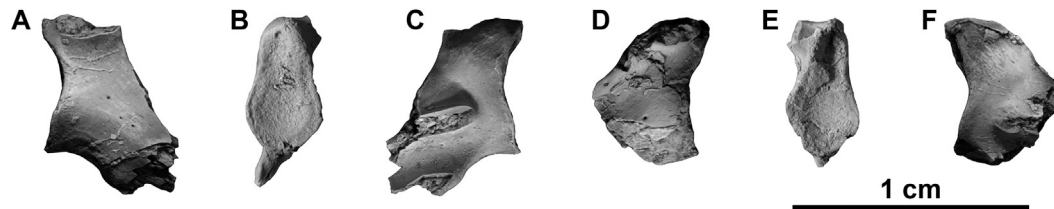


Figure 5. *Torrejonia wilsoni* (NMMNH P-54500) scapulae. A–C) Lateral portion of right scapula in ventral (A), lateral (B), and dorsal (C) views. D–F) Lateral portion of left scapula in ventral (D), lateral (E), and dorsal (F) views.

outline of the glenoid fossa of *T. wilsoni* is similar to that of many extant euarchontans such as treeshrews (Sargis, 2002a), *M. murinus*, and *C. volans*, as well as that of paromomyid and plesiadapid plesiadapiforms (e.g., Simpson, 1935; Beard, 1989; Boyer, 2009). The larger diameter of the convex humeral head compared to the concave glenoid fossa, along with other features of the proximal humerus (see below), indicate a mobile glenohumeral joint in *T. wilsoni*.

Humerus The humeri of *T. wilsoni* are quite similar to those of other known plesiadapiforms (see Szalay et al., 1975; Szalay and Dagosto, 1980; Beard, 1993; Bloch and Boyer, 2007; Bloch et al., 2007; Figs. 6 and 7). The left proximal epiphysis and a small proximal diaphyseal fragment, which fit together, are preserved. The humeral head is hemispherical and projects superiorly beyond the greater and lesser tuberosities (Fig. 6), which would have allowed considerable mobility at the glenohumeral joint. These well-developed tuberosities provide a great area of insertion for the rotator cuff muscles, which stabilize the shoulder joint of arboreal mammals that often have their forelimbs abducted (Sargis, 2002a). The greater tuberosity is positioned more superiorly than the lesser tuberosity, but it is not as prominent as that of plesiadapids (e.g., *P. cookei*; Boyer, 2009). The lesser tuberosity of *T. wilsoni* is robust, protrudes medially (Fig. 6F), and would have provided a long lever arm for *M. subscapularis* to medially rotate the humerus, as has been documented in extant vertical climbers such as many euprimates, the treeshrew *Ptilocercus lowii*, and colugos (Beard, 1991, 1993; Sargis, 2002a,b).

The left and right distal humeri are preserved with distal epiphyses fused, but a large portion of the diaphysis is missing on both sides. The diaphysis on the left side is slightly more complete and bears the distal most portion of the deltopectoral crest on the ventral surface, but it is unclear whether this entire crest would be positioned more ventrally as in colugos and treeshrews or more laterally as in most other plesiadapiforms and many euprimates. The left humerus preserves a prominent brachioradialis flange that flares dorsolaterally (Fig. 6K). This flange provides the origin for *M. brachioradialis* (and possibly *M. brachialis*), which would have contributed to forearm flexion. The deep radial fossa (Fig. 6A, K) would have allowed complete flexion of the antebrachium, and the shallow olecranon fossa (Fig. 6C, M) suggests limited extension of the antebrachium. The capitulum is spherical and has a prominent capitular tail (Fig. 6). Such a globular capitulum in *T. wilsoni* would have allowed a great degree of rotation of the radius, which would have resulted in a great capacity for supination and pronation of the forearm and hand (Szalay and Dagosto, 1980). The capitulum is separated from the trochlea by a distinct zona conoidea (Figs. 6A, K, 7A, C), which is defined by the groove between these two structures (Fig. 7C; Sargis, 2002a; Chester et al., 2010). The presence of a well-defined zona conoidea would have allowed the radius a greater freedom of movement relative to the ulna (Gebo and Sargis, 1994; Sargis, 2002a). The trochlea is short proximodistally but longer on the medial side and wasted laterally. This is a similar condition to that of plesiadapiforms such as the paromomyid *I. clarkforkensis*

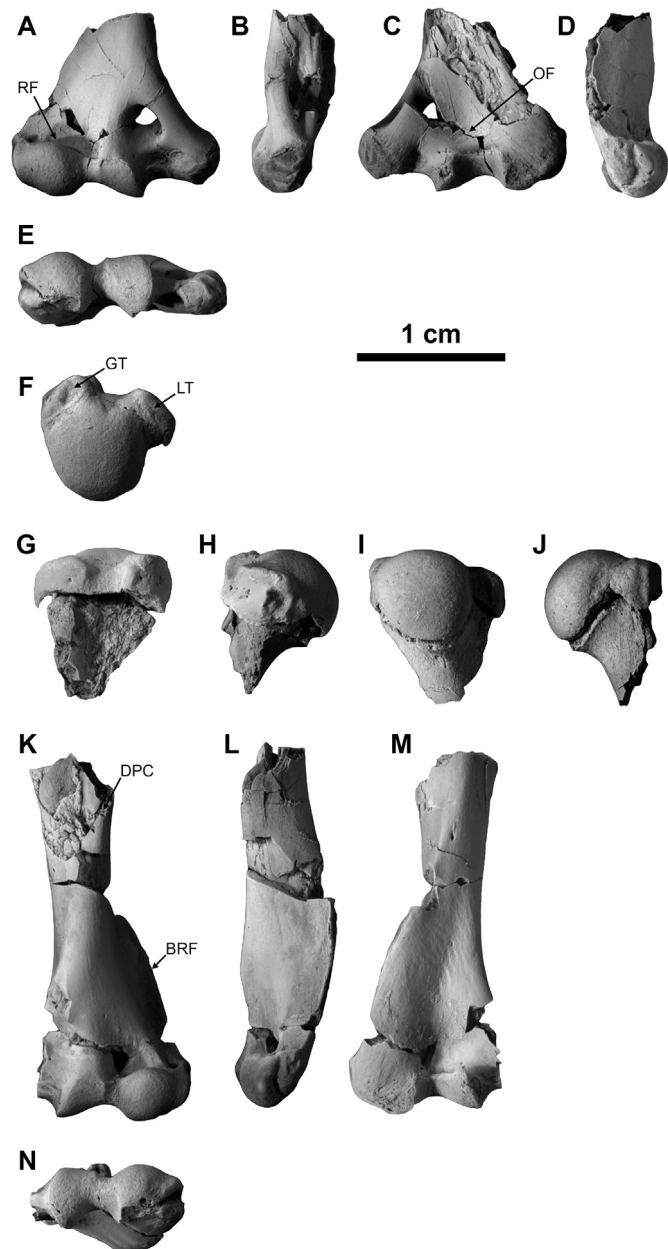


Figure 6. *Torrejonia wilsoni* (NMMNH P-54500) humeri. A–E) Distal end of right humerus in ventral (A), medial (B), dorsal (C), lateral (D), and distal (E) views. F–J) Proximal end of left humerus in proximal (F), ventral (G), lateral (H), dorsal (I), and medial (J) views. K–N) Partial left humerus in ventral (K), lateral (L), dorsal (M), and distal (N) views. Abbreviations: BRF = brachioradialis flange; DPC = deltopectoral crest; GT = greater tuberosity; LT = lesser tuberosity; OF = olecranon fossa; RF = radial fossa.

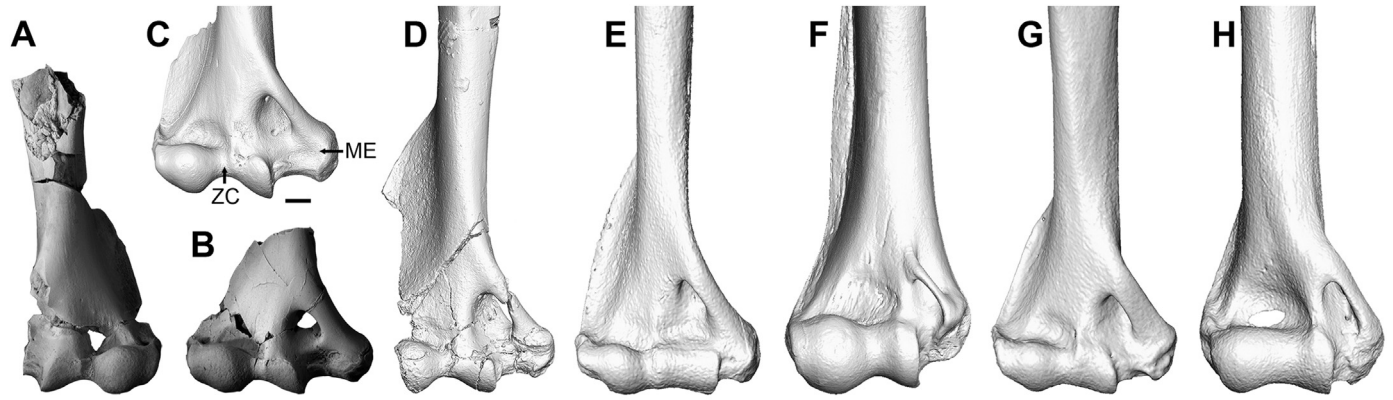


Figure 7. Photographs of left (A) and right (B) partial humeri of *Torrejonia wilsoni* (NMMNH P-54500) compared to renderings of 3D virtual models of distal humeri based on μ CT data of paromomyid plesiadapiforms cf. *Phenacolemur simonsi* (C; USNM 442260) and *Ignacius clarkforkensis* (D; UM 108210), extant euprimate *Galagoidea demidoff* (AMNH 269904; E), extant colugo *Cynocephalus volans* (ANSP 24797; F), extant treeshrews: arboreal *Ptilocercus lowii* (MCZ 51736; G) and terrestrial *Tupai gracilis* (FMNH 140928; H) in ventral view. Abbreviations: ME = medial epicondyle; ZC = zona conoidea. Specimens scaled to width of distal end. Scale bars = 1 mm. Some elements reversed to facilitate comparisons. Modified from Chester et al. (2017:Fig. 2).

(as well as to that of an isolated humerus attributed to *Phenacolemur simonsi*; Beard, 1993; Fig. 7), whereas the extant arboreal treeshrew, *Ptilocercus*, exhibits a humeral trochlea with a lateral side that is more similar in length to that of the medial side (Fig. 7; Sargis, 2002a:Fig. 11). An entepicondylar foramen is present proximal to a very wide medial epicondyle in *T. wilsoni*, which represents just over one third of the maximum distal width of the humerus (Fig. 6A, C, E; Table 1). The width of the medial epicondyle is similarly expansive to that of plesiadapiforms such as *I. clarkforkensis* (and an isolated humerus attributed to *Ph. simonsi*; Beard, 1993; Fig. 7) and would have provided a large area of origin for the wrist and digital flexors for manual grasping in the branches of trees (Argot, 2001; Sargis, 2002a). However, the medial epicondyle of *T. wilsoni* is not as wide relative to the width of the distal end compared to that of *Carpolestes simpsoni*, which appears to be one of many carpolestid postcranial specializations for more powerful grasping of smaller diameter supports in a fine branch niche (Bloch and Boyer, 2002, 2007).

Overall, the humeral features of *T. wilsoni* suggest mobile shoulder and elbow joints with habitual flexion at the elbow and capability of manual grasping as required for climbing and clinging on vertical supports. When comparing the humeri of *T. wilsoni* to those of other plesiadapiforms and euarchontan mammals, this palaechthonid is most similar overall to *I. clarkforkensis* and to the isolated humerus previously attributed to *Ph. simonsi* (Fig. 7).

Ulna Both proximal ulnae have fused epiphyses but are broken across the trochlear notch, and the remainder of the diaphyses are not preserved (Fig. 8A–D). The olecranon processes are short and appear to be straight. The ulna of *T. wilsoni* also appears to have a shallow trochlear notch like that of other plesiadapiforms. The medial side of the proximal end is also like that of other plesiadapiforms in being deeply excavated (Fig. 8D), probably relating to the origin of *M. flexor carpi ulnaris*; this muscle would have contributed to flexion and adduction of the wrist. Both ulnae only preserve the most proximal aspect of the radial notch, and based mostly on the left proximal ulna, it appears as though it would have been flat and slightly concave, allowing greater mobility of the radius relative to the ulna. A right distal epiphysis with a globular styloid process is preserved and attributed to *T. wilsoni* (Fig. 8E–I). The ulna is not fused to the radius distally as it is in colugos.

Radius Both proximal radii are preserved with the proximal epiphyses fused and diaphyses that are broken slightly distal to the

bicipital tuberosities (Fig. 8J–N). Given the morphology of the distal humeral articular surfaces of *T. wilsoni*, it is not surprising that the morphology of the proximal radii also indicates a great deal of mobility at the elbow joint. The radial head of *T. wilsoni* is ovoid in proximal view (Fig. 8N), which differs from the more circular outline exhibited in plesiadapiforms such as *I. clarkforkensis*. However, the central fossa of *T. wilsoni* is round and excavated, and the radial head rim for articulation with the radial notch of the ulna is extensive (Fig. 8L, M), allowing the radius to move more freely on the spherical capitulum as in euprimates, colugos, *Pt. lowii*, and other plesiadapiforms (Sargis, 2002b). The bicipital tuberosity is large and proximally located, suggesting the presence of a large *M. biceps brachii*, a flexor and supinator of the antebrachium that would have contributed to climbing (Argot, 2001; Sargis, 2002a).

A right distal radial epiphysis is also preserved (Fig. 8O). It has a shallowly concave distal articular surface that is deeper on the dorsal side than on the ventral side. The distal-most portions of the styloid process and dorsal tubercle are preserved with the distal articular surface, which is cupped. However, the presence or absence of a ventrally (i.e., anteriorly)-canted articular surface in *T. wilsoni*, as observed in micromomyid plesiadapiforms, *Pt. lowii*, and colugos (Boyer and Bloch, 2008), cannot be assessed from the epiphysis in isolation. Overall, the rather shallow condition of the distal articular surface suggests a mobile radiocarpal joint.

Innominates The partial right innominate of *T. wilsoni* is quite similar to that of other plesiadapiforms and extant arboreal euarchontans (Figs. 9 and 10). A large portion of the acetabular fossa is missing, but enough of the acetabulum is preserved to see that it had a craniocaudally elliptical shape (Fig. 9B) as in extant arboreal euarchontans and other plesiadapiforms, such as paromomyids or isolated elements attributed to the micromomyid *Ti. graybulliensis* (Beard, 1991, 1993; Sargis, 2002b,c; Boyer and Bloch, 2008; Fig. 10). Such an elliptical acetabulum in *T. wilsoni* would have allowed great mobility at the hip joint for wide ranges of abduction and lateral rotation, which is important for arboreal climbers, such as many euprimates, colugos (Fig. 10E; Beard, 1991), and *Pt. lowii* (Fig. 10F; Sargis, 2002c). This condition contrasts with the circular-shaped acetabulum of terrestrial treeshrews (Fig. 10G; Sargis, 2002c). As in other extant arboreal euarchontans and plesiadapiforms, the bony buttressing and expanded articular surface on the cranial aspect of the acetabulum of *T. wilsoni* likely reflects loads that

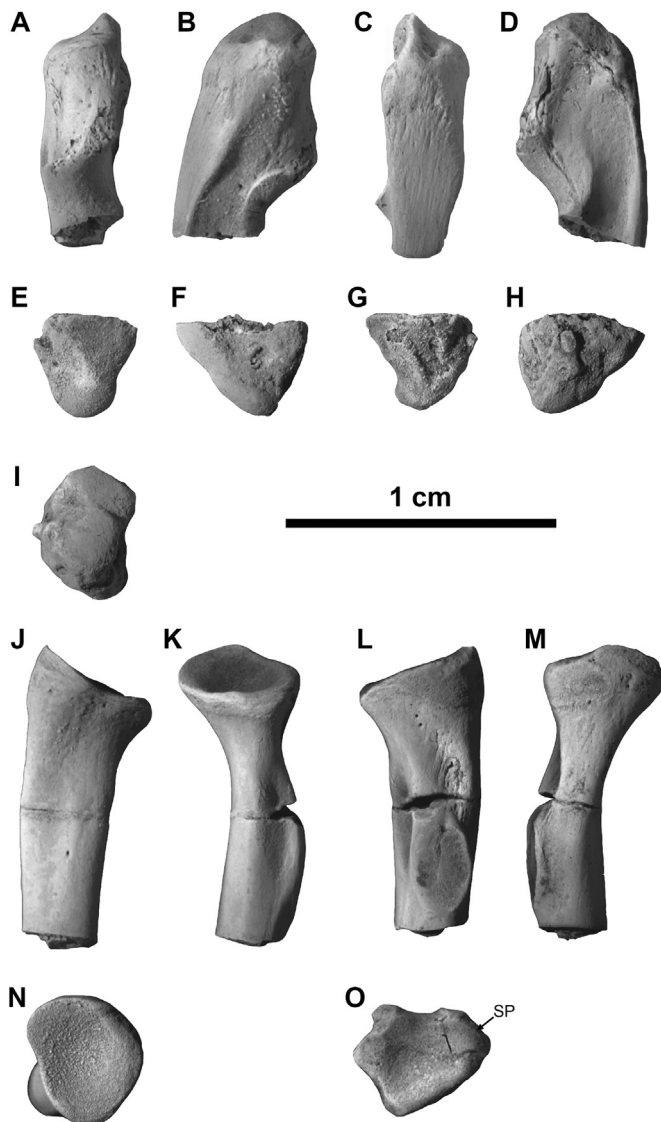


Figure 8. *Torrejonia wilsoni* (NMMNH P-54500) ulna and radius. A–D) Right proximal ulna in ventral (A), lateral (B), dorsal (C), and medial (D) views. E–I) Right distal ulnar epiphysis in ventral (E), lateral (F), dorsal (G), medial (H), and distal (I) views. J–N) Right proximal radius in dorsal (J), lateral (K), ventral (L), medial (M), and proximal (N) views. O) Right distal radial epiphysis in distal view. Abbreviation: SP = styloid process.

were incurred during orthograde positional behaviors on vertical supports (Beard, 1991). These features of the innominate are not present in terrestrial tupaids (Fig. 10G; Sargis, 2002c). *Torrejonia wilsoni* also has a small anterior inferior iliac spine (Figs. 9, 10A) as in other arboreal euarchontans (Sargis, 2002b,c). This would have provided a small origin for *M. rectus femoris* in *T. wilsoni* unlike the large anterior inferior iliac spine in terrestrial treeshrews, which is related to powerful leg extension during terrestrial running (Sargis, 2002c; Fig. 10G).

Femur The right and left proximal femora and left tibia are adhered together in a calcareous concretion (Fig. 11A–B). The femora of *T. wilsoni* are missing their proximal epiphyses, so the height of the greater trochanter relative to the head is unknown. However, it is clear that like those of other plesiadapiforms, the femora of *T. wilsoni* have short necks (Fig. 12). Though still partially covered in matrix, the trochanteric fossa of the right femur appears long and deep (Fig. 11A). Two obturator and two gemelli muscles insert in this fossa and would have contributed to lateral rotation

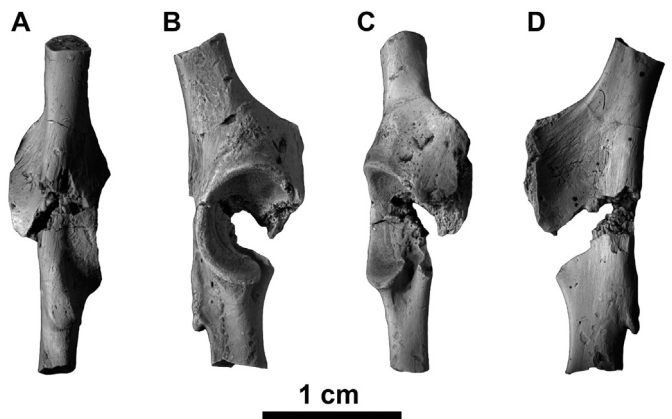


Figure 9. A–D) *Torrejonia wilsoni* (NMMNH P-54500) right partial innominate in dorsal (A), lateral (B), ventral (C), and medial (D) views.

of the thigh when using vertical supports. The lesser trochanter is broken on the left femur, but the right femur preserves one that is large and oriented dorsomedially, as in other plesiadapiforms (Fig. 12). The large lesser trochanter provides a large area of insertion for *M. iliopsoas*, which contributes to hip flexion (Bloch and Boyer, 2007). However, the lesser trochanter of *T. wilsoni* appears to be located slightly more proximally than that of the paromomyid *I. clarkforkensis* (Fig. 12B), and may be more similar in position to that of a femur attributed to the micromomyid *Ti. graybulliensis* (Fig. 12C; Beard, 1993). Both femora of *T. wilsoni* preserve the third trochanters, which are abraded and distorted from dorsoventral compression, yet were clearly small, positioned distal to the lesser trochanter, and laterally projecting. The fairly small third trochanter indicates a small attachment area for *M. gluteus superficialis*. This suggests that *T. wilsoni* was not powerfully extending its thigh like specialized terrestrial runners or leapers and instead had hind limbs that were often flexed (Sargis, 2002c; Chester et al., 2012). The condition of *T. wilsoni* contrasts, for example, with the large third trochanter in the terrestrial treeshrew *T. gracilis* (Fig. 12G).

The left distal epiphysis and a diaphyseal fragment fit together (Fig. 11C–G). A less complete right distal diaphyseal fragment is also preserved along with an isolated lateral condyle. The distal ends of the femora are fairly shallow dorsoventrally (Fig. 12A), unlike the deeper condyles of leaping euprimates (Fig. 12D). Terrestrial treeshrews also differ from *T. wilsoni* in having deeper condyles (Fig. 12G) because greater depth increases the leverage of *M. quadriceps femoris* for extending the leg during terrestrial locomotion (Sargis, 2002c). Like colugos, *Pt. lowii*, and other plesiadapiforms (Szalay et al., 1975; Beard, 1989, 1993; Sargis, 2002b,c; Fig. 12), *T. wilsoni* also has a shallow, wide, and proximally restricted patellar groove, which is indicative of less extensive excursion of the knee and suggests a more habitually flexed posture (Sargis, 2002c). *Torrejonia wilsoni* therefore was probably not powerfully extending its knee as running and leaping specialists do (Beard, 1989; Sargis, 2002c). The condyles are similar to one another in width as in other eutherians (e.g., Szalay and Sargis, 2001; Sargis, 2002c; Chester et al., 2012), but the lateral condyle is slightly wider than the medial one (Fig. 11G).

Tibia The tibiae of *T. wilsoni* are fairly complete, though the proximal epiphyses from both sides are missing (Fig. 11H–L). They appear to lack a large tibial crest and tuberosity, which probably also indicates a habitually flexed knee without much capability for powerful extension (Sargis, 2002c). The diaphysis is bowed ventrally and the distal end is curved medially (Fig. 11H), which would have made the feet somewhat inverted when flexed (Bloch

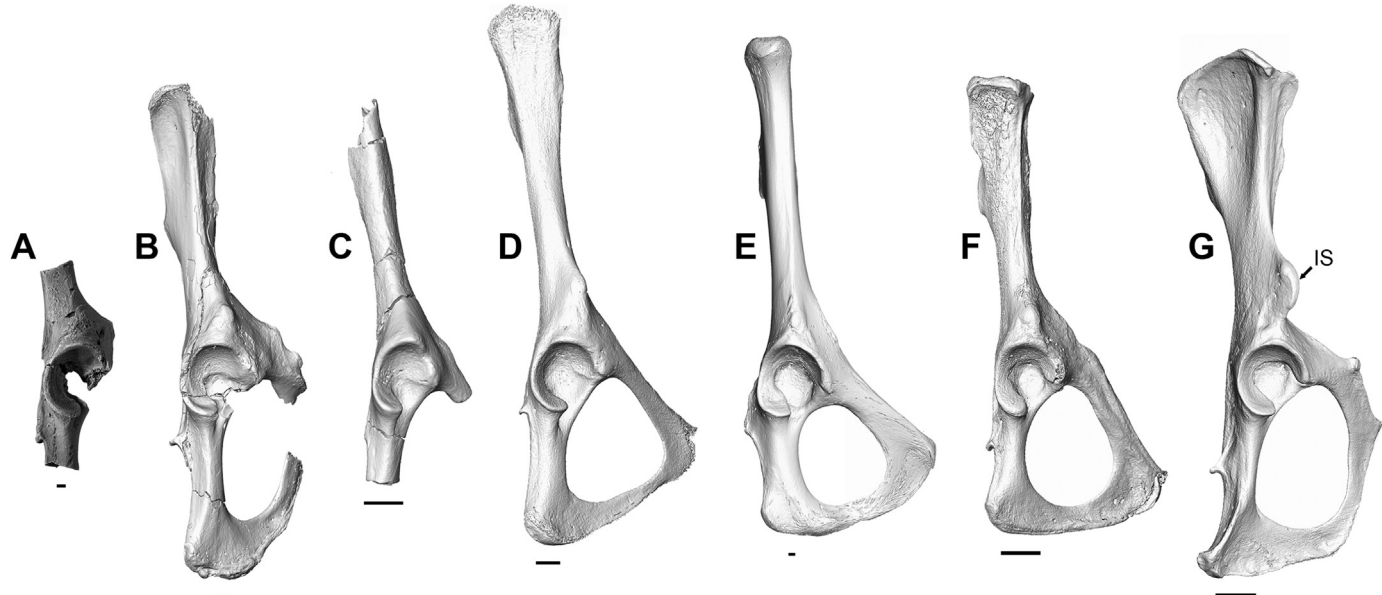


Figure 10. Photograph of partial right innominate of *Torrejonia wilsoni* (NMMNH P-54500; A) compared to renderings of 3D virtual models of innomates based on μ CT data of paromomyid plesiadapiform *Ignacius clarkforkensis* (UM 82606; B), micromomyid plesiadapiform cf. *Tinomomys graybulliensis* (USNM 442277; C), extant euprimate *Galagooides demidoff* (AMNH 269904; D), extant colugo *Cynocephalus volans* (ANSP 24797; E), extant tree shrews: arboreal *Ptilocercus lowii* (MCZ 51736; F) and terrestrial *Tupaia gracilis* (FMNH 140928; G) in lateral view. Abbreviations: IS = anterior inferior iliac spine. Specimens scaled to craniocaudal length of acetabulum. Scale bars = 1 mm. Some elements reversed to facilitate comparisons. Modified from Chester et al. (2017:Fig. 2).

and Boyer, 2007). The right distal epiphysis is fused to the diaphysis, but the epiphyseal line is still present (Fig. 11H–K). As in other plesiadapiforms, the medial malleolus is short and the astragalar facet of the tibia is ungrooved and angled dorsolaterally, which mirrors the morphology of the lateral tibial facet of the astragalus (see below). The malleolar groove is fairly shallow, yet distinct, for transmission of the tendons of *M. flexor digitorum tibialis* and *M. tibialis posterior* (Fig. 11J). *Flexor digitorum tibialis* is crucial for grasping and *tibialis posterior* is important for inverting the foot.

Fibula There is a partial diaphysis preserved in association with the right and left femora and left tibia (Fig. 11A). It is considerably smaller in diameter than these other bones, ovoid in cross section, and likely represents the fibula of *T. wilsoni*.

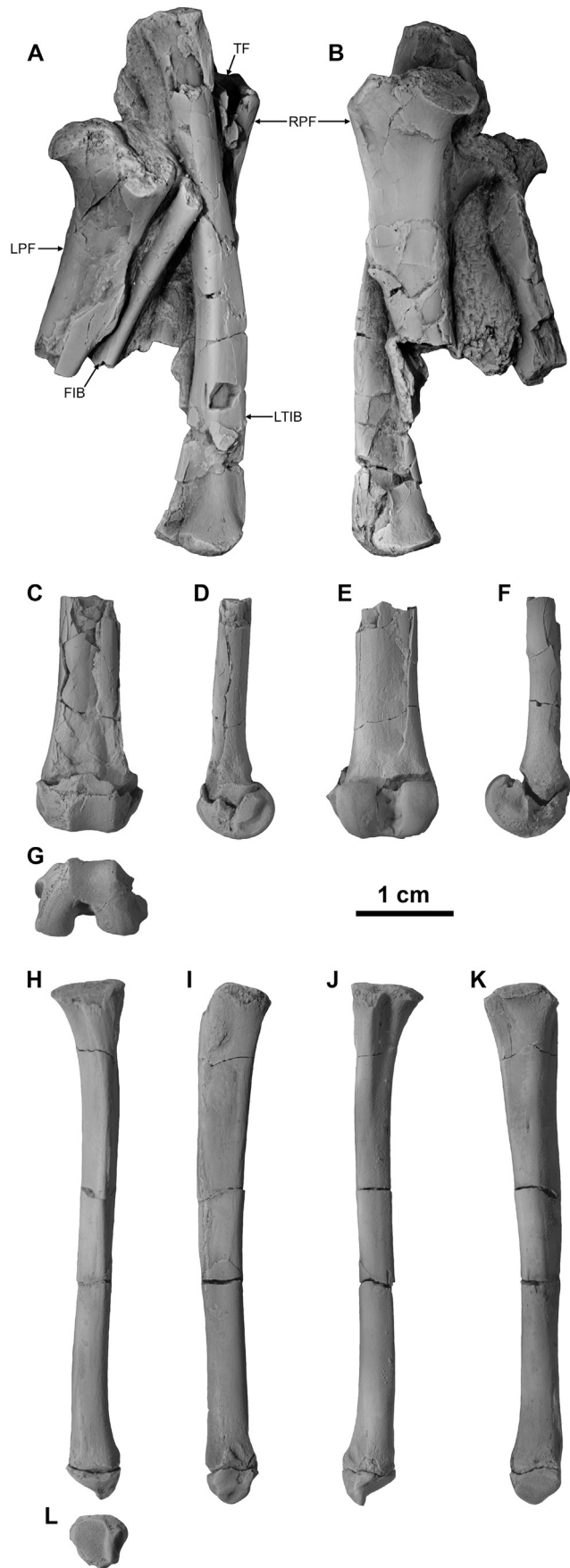
Astragalus Many tarsal features of plesiadapiforms and other arboreal euarchontans relate to mobility of the foot, permitting a wide range of inversion and eversion to adjust to uneven and variable substrates (Szalay and Decker, 1974; Szalay and Drawhorn, 1980). NMMNH P-54500 preserves the body of the right astragalus (Fig. 13A–F). The lateral tibial facet extends at least slightly onto the dorsal surface of the neck (squatting facet; Fig. 13A), which reflects habitual dorsiflexion of the foot that is typical of mammals that cling to the sides of vertical supports such as tree trunks (Szalay and Drawhorn, 1980). The lateral tibial facet is very shallowly grooved and has weak trochlear ridges (Fig. 13F). As in other plesiadapiforms, the lateral trochlear crest is relatively taller and more distinct than the medial one (Fig. 14). However, the medial trochlear crest is defined, which is also true of astragali of micromomyids (Fig. 14D) and those attributed to *Purgatorius* (Fig. 14C; Chester et al., 2015). The presence of a fairly tall medial trochlear crest contributes to a lateral tibial facet that does not slope as steeply medially as the likely more derived conditions of certain paromomyids and plesiadapids (Fig. 14E, F). This condition of *T. wilsoni* also contrasts with the lack of distinct trochlear ridges on the astragalus of *Ca. simpsoni* (Fig. 14G), which would have had a more mobile upper ankle joint (Bloch and Boyer,

2007). The lateral trochlear ridge of *T. wilsoni* ends proximally at a small superior astragalar foramen (Fig. 13A,E).

The lateral side of the astragalar body consists of a convex fibular facet that forms an obtuse angle with the lateral tibial facet. The fibular facet is positioned dorsal and distal to a depression for attachment of the astragalarfibular ligament (Fig. 13B). The medial trochlear crest creates an angle between the lateral and medial tibial facets that is slightly obtuse. The flexor fibularis groove on the astragalus is not as relatively large and wide as that of micromomyids (Fig. 14D) or that attributed to *Purgatorius* (Fig. 14C; Chester et al., 2015) and is more similar to the condition in paromomyids such as *I. clarkforkensis* (Fig. 14E; Boyer and Bloch, 2008:Fig. 11.4). *Torrejonia wilsoni* has a concave ectal facet that is larger than the flexor fibularis groove and oriented obliquely (proximomedially to distolaterally) to the long axis of the astragalus (Fig. 13C). The ectal facet is separated from the sustentacular facet by the sulcus astragali, which leads proximomedially to the inferior astragalar foramen. The sustentacular facet is very abraded and mostly missing because the astragalar neck is not preserved, but the articular surface that would have contacted the small proximal facet of the sustentaculum tali (on the calcaneus) is preserved. The astragalar sustentacular facet likely continued distally and was confluent with the navicular facet, given that the corresponding sustentacular facet of the associated calcaneus continues distally onto the body (Fig. 13G), as in other plesiadapiforms and many euarchontans (Fig. 14; Szalay and Drawhorn, 1980).

Overall, the body of the astragalus of *T. wilsoni* is most similar to that of other plesiadapiforms such as the paromomyid *Ignacius* and the micromomyid *Dryomomys* among euarchontans (Fig. 14). It appears to be intermediate between micromomyids and paromomyids regarding how steeply the lateral tibial facet slopes medially, and more similar to paromomyids regarding the width of the groove for flexor fibularis.

Calcaneus NMMNH P-54500 preserves the complete right calcaneus (Fig. 13G–L), which is similar to that of other plesiadapiforms, and articulates well with the right astragalar body described above.



The calcaneal tuber and ectal facet make up approximately two-thirds of the complete length, and the calcaneus is not nearly as distally elongate as that of many early euprimates or that of *Ca. simpsoni* (see Boyer et al., 2013b; Fig. 14). The ectal facet is knuckle-shaped, convex medially, and oriented approximately 25° distolaterally to the long axis of the bone. The ectal facet on the calcaneus is slightly longer than the corresponding ectal facet on the astragalus, and manual articulation of these bones clearly demonstrates that translation could have occurred at the lower ankle joint.

The proximal sustentacular facet is oriented slightly distolaterally and located on a large, medially projecting sustentaculum tali, which is separated from the ectal facet by an interosseus sulcus. The plantar side of the sustentaculum has a wide but fairly shallow groove for the tendon of *M. flexor fibularis* (Fig. 13I–J). The proximal sustentacular facet continues distally on the calcaneal body to the dorsomedial border of the cuboid facet. This suggests that movements between the astragalus and calcaneus would have also occurred at the distal end of the lower ankle joint, which ultimately would have resulted in a wide range of inversion and eversion at this joint (Szalay and Decker, 1974; Szalay and Drawhorn, 1980). There is also a small proximal facet on the sustentaculum tali (Fig. 13G, K) that would have articulated with the proximal aspect of the astragalar sustentacular facet during maximum inversion and increased stability at the lower ankle joint (Beard, 1989, 1993).

One of the most striking features of the calcaneus is the very large peroneal tubercle, which projects distolaterally and is positioned on the lateral side, mostly distal to the distal-most aspect of the ectal facet (Fig. 13G). Such a large and distally projecting peroneal tubercle would provide considerable leverage for tendons of muscles that evert and invert the foot (Szalay and Decker, 1974; Gunnell, 1989). There is a shallow groove on the lateral side of the peroneal tubercle for the placement of the tendon of *M. peroneus longus*, which would have contributed to pedal eversion (Fig. 13H). The large peroneal tubercle would have also provided room dorsally for the tendon of *M. peroneus brevis* and plantarly for *M. abductor digiti quinti* (Szalay and Decker, 1974), which would have contributed to pedal eversion and abduction of the fifth digit, respectively.

Unlike the conditions of many other plesiadapiforms, including calcanei attributed to *Purgatorius* (Fig. 14C; Chester et al., 2015), the peroneal tubercle of *T. wilsoni* extends farther distally on the lateral side and the cuboid facet is oriented more obliquely medially (Fig. 14). The calcaneus of *T. wilsoni* is more similar to one attributed by Prasad and Godinot (1994) to *Deccanolestes hislopi* in these features, but is still even more pronounced in these ways. These conditions are also present in tarsals attributed to the earliest Paleocene archaic ungulate *Protungulatum* (Fig. 14B) and have been proposed to characterize the eutherian morphotype (Szalay and Decker, 1974; but see Prasad and Godinot, 1994).

The cuboid facet of *T. wilsoni* is subcircular in outline (Fig. 13L). Although it is not as circular in outline as that of many plesiadapiforms, it is relatively deeper dorsoplantarly and considerably more concave than that of calcanei attributed to *Protungulatum* (Fig. 14). The cuboid facet also has a well-developed pit on the

Figure 11. *Torrejonia wilsoni* (NMMNH P-54500) femora and tibiae. A, B) Concretion with left and right proximal femora, partial left tibia, and partial fibular diaphysis in two views. C–G) Left distal femur in ventral (C), lateral (D), dorsal (E), medial (F), and distal (G) views. H–L) Right tibia missing proximal epiphysis in ventral (H), medial (I), dorsal (J), lateral (K), and distal (L) views. Abbreviations: FIB = partial fibular diaphysis; LPF = left proximal femur; LTIB = partial left tibia; RPF = right proximal femur; TF = trochanteric fossa.

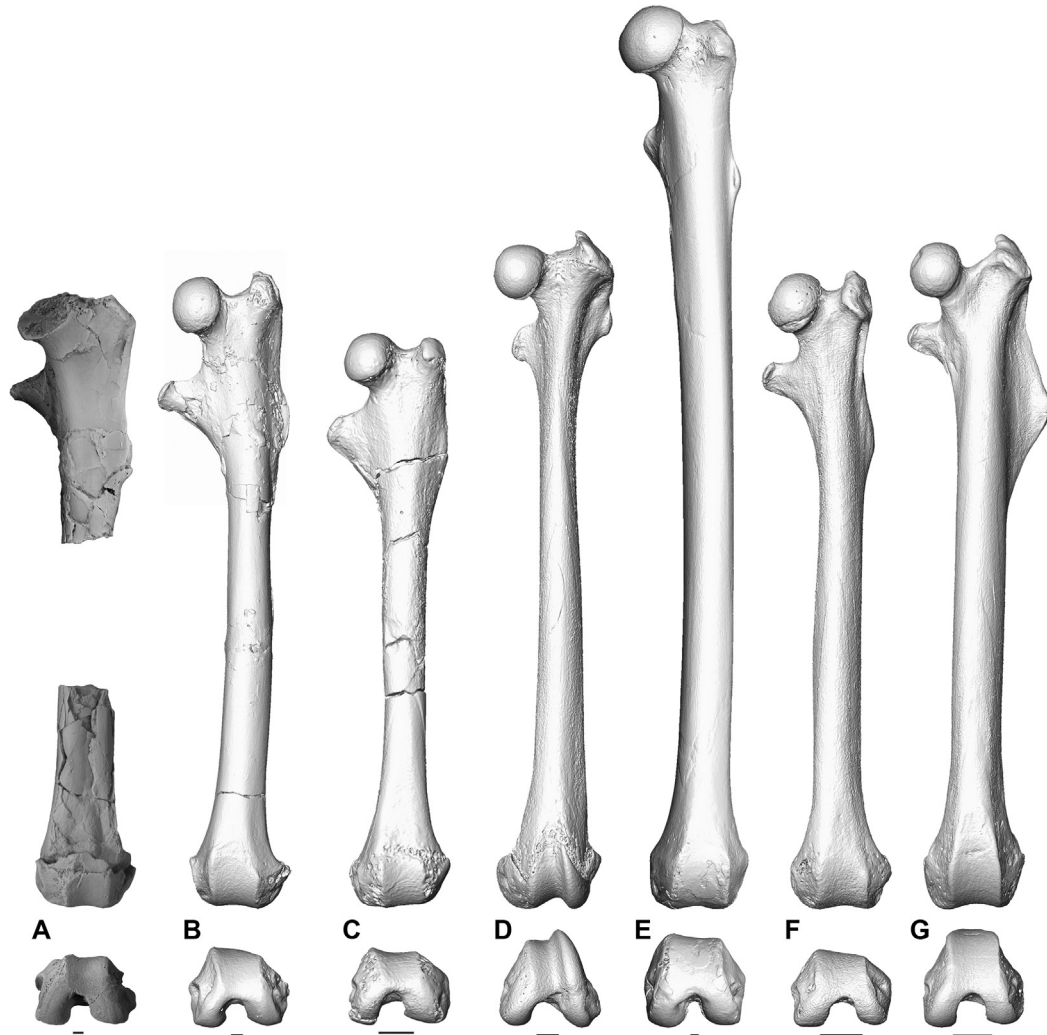


Figure 12. Photographs of partial right femur (reversed and cropped from Fig. 11B) and left distal femur of *Torrejonia wilsoni* (NMMNH P-54500; A) compared to renderings of 3D virtual models of femora based on µCT data of paromomyid plesiadapiform *Ignacius clarkforkensis* (UM 82606; B), micromomyid plesiadapiform cf. *Tinimomys graybulliensis* (USNM 442280; C), extant euprimate *Galagooides demidoff* (AMNH 269904; D), extant colugo *Cynocephalus volans* (ANSP 24797; E), extant treeshrews: arboreal *Ptilocercus lowii* (MCZ 51736; F) and terrestrial *Tupaiia gracilis* (FMNH 140928; G) in ventral (above) and distal (below) views. Specimens scaled to width of distal end. Scale bars = 1 mm. Some elements reversed to facilitate comparisons. Modified from Chester et al. (2017:Fig. 2).

plantar side just distal to the anterior plantar tubercle (Fig. 13I, L), which would have allowed the cuboid to rotate more freely on the calcaneus during inversion and eversion (Szalay and Drawhorn, 1980).

Overall, the calcaneal morphology of *T. wilsoni* is somewhat surprising in that it retains likely primitive conditions including the distal position of the peroneal tubercle and oblique orientation of the cuboid facet, similar to that of the archaic ungulate *Protungulatum*. However, *T. wilsoni* is similar to other plesiadapiforms and differs from *Protungulatum* in having derived conditions for more inversion at the lower ankle and transverse tarsal joints. Such features include an ectal facet more in line with the long axis of the calcaneus, a more extensive sustentacular articular surface on the distal aspect of the body, and a deeper and more concave cuboid facet.

Cuboid The cuboids of *T. wilsoni* are preserved intact in NMMNH P-54500 (Fig. 13M–R). They are rectangular in shape with a proximal articular surface (Fig. 13Q) that mirrors the cuboid facet of the calcaneus (Fig. 13L). The proximal articular facet of the cuboid has a convex apex on the plantar side that articulates with the plantar pit of the calcaneus and is quite extended distolaterally in

relation to the distolateral margin of the cuboid facet (Fig. 13N). Like that of other plesiadapiforms, the plantar side of the cuboid has a pronounced groove that runs mediolaterally (Fig. 13O) to transmit the tendon of *M. peroneus longus*, an evertor of the foot (see above; Bloch and Boyer, 2007). The distal articular surface (Fig. 13R) is triangular in outline and slightly concave for articulation with the proximal ends of the fourth and fifth metatarsals.

Metapodials and phalanges Several metapodials and phalanges within the expected size range of *T. wilsoni* and *A. secans* were recovered from locality NMMNH L-6898, but as is the case with the partial vertebrae and sternebrae recovered from this site (see above), almost all of these elements are fragmentary, they were not found articulated or closely associated, and they cannot be attributed to the partial skeleton of *T. wilsoni* with confidence at this time. A fifth metacarpal, a proximal phalanx, and a partial intermediate phalanx are described below and tentatively attributed to *T. wilsoni* based on their similarities to those of other plesiadapiforms. There is currently not enough information to assess prehensile capabilities based on the relative length of the recovered metapodials, proximal phalanges, and intermediate phalanges, and

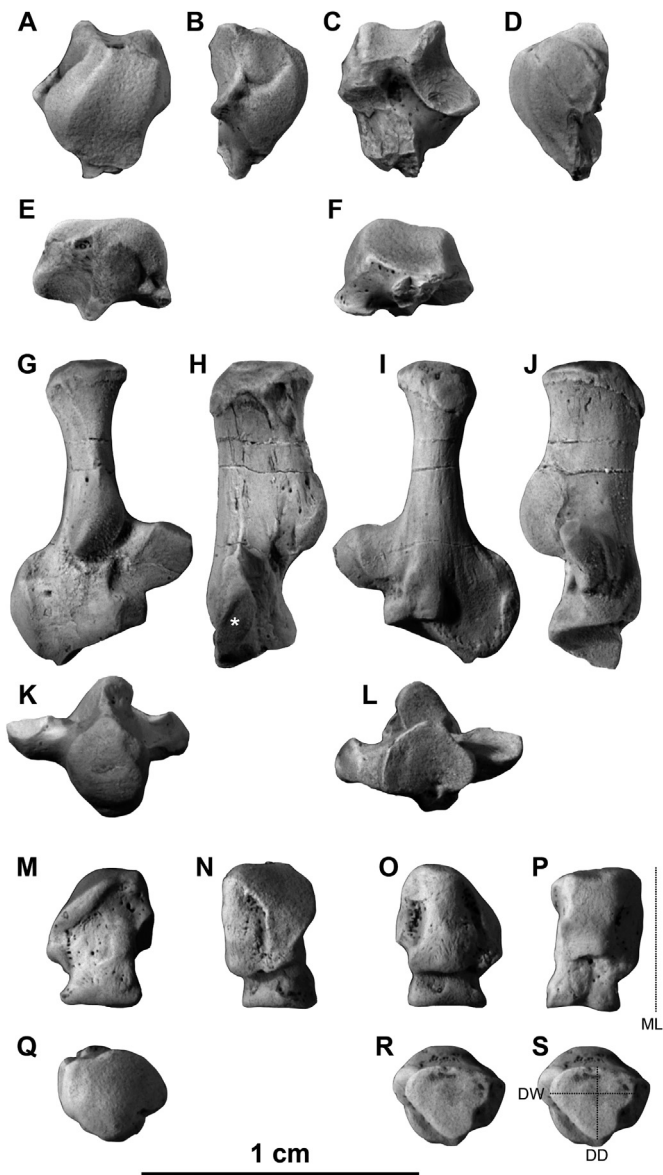


Figure 13. *Torrejonia wilsoni* (NMMNH P-54500) tarsals. A–F) Right astragalar body in dorsal (A), lateral (B), plantar (C), medial (D), proximal (E), and distal (F) views. G–L) Right calcaneus in dorsal (G), lateral (H), plantar (I), medial (J), proximal (K), and distal (L) views. M–R) Right cuboid in dorsal (M), lateral (N), plantar (O), medial (P), proximal (Q), and distal (R, S) views. White asterisk = shallow groove for tendon of *M. peroneus longus*. Dotted black lines illustrate the following measurements (see Table 2): ML = Cuboid maximum proximodistal length; DD = Cuboid distal facet dorsoplantar depth; DW = Cuboid distal facet mediolateral width.

no distal phalanges recovered at this site are within the expected size range of *T. wilsoni*.

A right fifth metacarpal (MC5; Fig. 15A–F) is tentatively attributed to *T. wilsoni* based on its similarity to that of micromomyid and plesiadapid plesiadapiforms (see Boyer et al., 2013a:Fig. 6). It is similar to the MC5 of the micromomyid *D. szalayi* and the plesiadapid *Nannodectes intermedius* in the shape of the head and base, although it has a slightly more robust shaft. As has been documented in other plesiadapiforms and many euprimates, the metacarpal head is spherical, which would have allowed considerable mobility for an arboreal mammal (Boyer et al., 2016). The distal articular surface of the metacarpal faces dorsally (Fig. 15B), which may have promoted hyperextension at the

metacarpophalangeal joint, as has been interpreted for plesiadapiforms (Godinot and Beard, 1991; Boyer et al., 2013a, 2016).

A proximal phalanx (Fig. 15G–L) is also tentatively attributed to *T. wilsoni* based on its similarity to that of known plesiadapiforms (Godinot and Beard, 1991; Boyer and Bloch, 2008; Boyer et al., 2013a, 2016). It is fairly large relative to the MC5 described above, so it is likely a pedal phalanx. The shaft is curved, and on the distal part there are well-demarcated flexor sheath ridges, which are very similar in size and position to those of other plesiadapiforms. These ridges are for the attachment of annular ligaments that help prevent bowstringing of the flexor tendons, which contribute to grasping (Bloch and Boyer, 2007). The proximal articular surface of the proximal phalanx faces proximodorsally (Fig. 15H), as in other plesiadapiforms, which may have promoted hyperextension at the metatarsophalangeal joint (Godinot and Beard, 1991; Boyer et al., 2013a, 2016). The distal articular surface has a central groove separating the medial and lateral margins, which closely mirrors the proximal articular surface of a partial intermediate phalanx (Fig. 15Q) and is similar to that of other plesiadapiforms (Godinot and Beard, 1991; Boyer et al., 2013a, 2016). Though the partial intermediate phalanx (Fig. 15M–Q) is missing its distal end and its curvature cannot be adequately assessed, it is quite similar to the condition present in other plesiadapiforms in having a shaft that tapers distally and a proximal articular surface with subequal maximum width and depth dimensions that is approximately triangular in proximal view due to its relatively narrow dorsal apex (Boyer et al., 2013a, 2016).

4. Discussion

Palaeochthonids have played an important role in debates regarding the paleobiology of the oldest and most primitive primates. Kay and Cartmill (1974, 1977) used *P. nacimenti* as a model of the ancestral primate. It was the oldest plesiadapiform known at the time represented by dental and cranial remains and its cranial morphology appeared more plesiomorphic than that of other known plesiadapiforms. Its dentition, like that of other palaeochthonids, shares a number of primitive similarities with the oldest known plesiadapiform, *Purgatorius*, including possibly the retention of I_3 (Silcox, 2001:Fig. 3.3). More recently discovered and more complete plesiadapiform fossils show that several craniodental features used by Kay and Cartmill (1974, 1977) to infer that *P. nacimenti* was primarily terrestrial (e.g., relatively large infraorbital foramina and small orbits that are oriented laterally) are present in arboreal plesiadapiforms such as the micromomyid *D. szalayi* (Bloch et al., 2007, 2016). Recent analyses demonstrate that plesiadapiforms such as the paromomyid *Ignacius* had large olfactory bulbs (Silcox et al., 2009), which implies more emphasis on olfaction and less on vision, and is consistent with the inferences made by Kay and Cartmill (1974, 1977)—but, again, associated skeletons show that these taxa were arboreal (Bloch et al., 2007; Boyer and Bloch, 2008). Furthermore, Szalay (1981) noted that many of the craniodental features hypothesized to be related to terrestriality are also present to varying degrees in *Pt. lowii*, the arboreal and most basally-divergent extant treeshrew, which may be the best extant model for the ancestor of Euarchonta (Bloch et al., 2007).

The partial skeleton of *T. wilsoni* described here allows the opportunity to directly evaluate the postcranial morphology of a palaeochthonid plesiadapiform. The forelimb of *Torrejonia* provides evidence for a mobile shoulder, a habitually flexed forearm, considerable supination and pronation of the forearm and hand, and manual grasping. The hind limb provides evidence for wide ranges of abduction and lateral rotation at the hip joint, a habitually flexed thigh and knee, and mobile ankle joints for inversion and eversion. Overall, *Torrejonia* is reconstructed as an arboreal climber

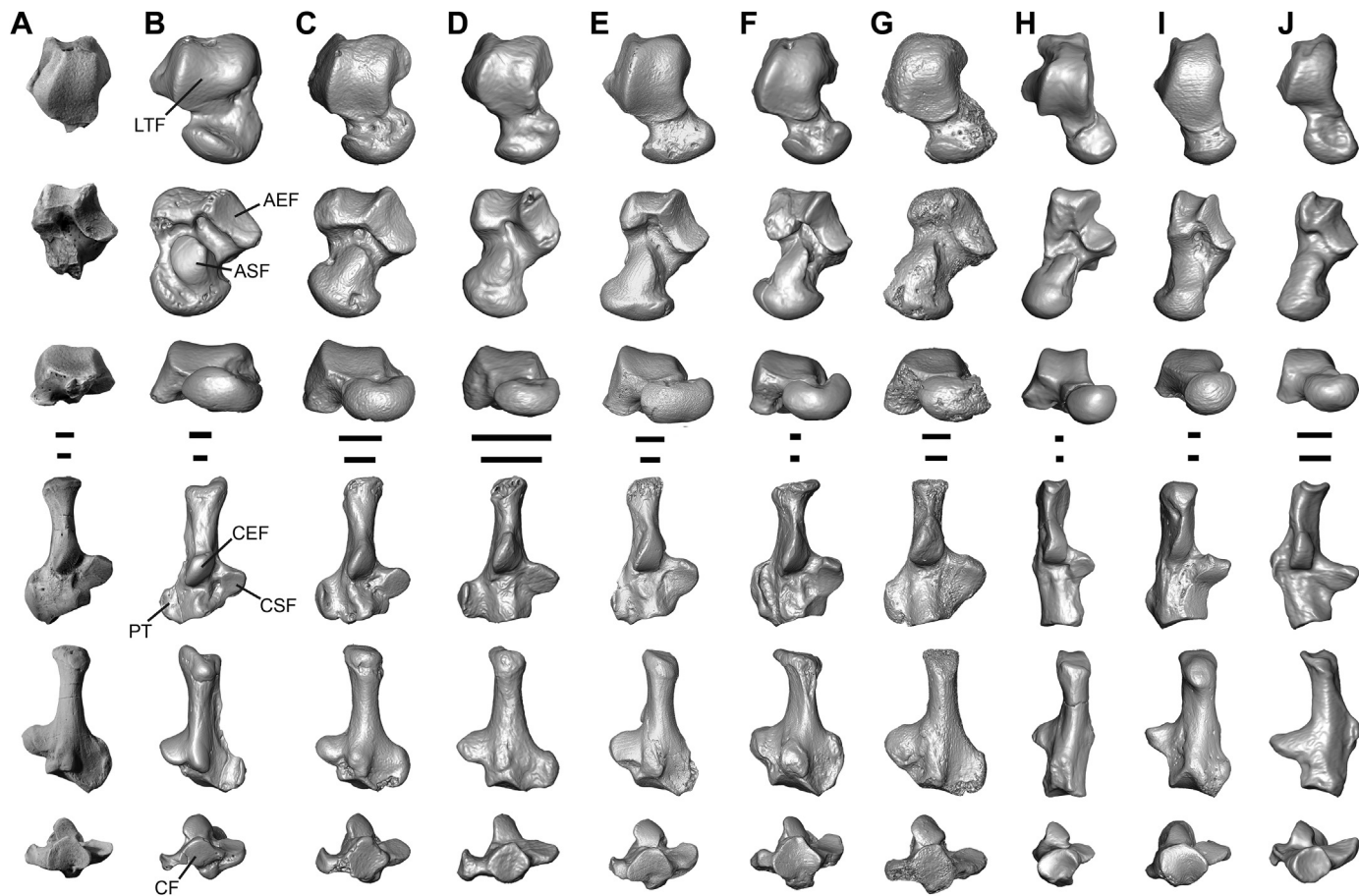


Figure 14. Photographs of partial right astragali and complete calcaneus of *Torrejonia wilsoni* (NMMNH P-54500; A) compared to renderings of 3D virtual models based on μ CT data of astragali and calcanei of archaic ungulate cf. *Protungulatum* (AMNH 118260, 118060; B), purgatoriid plesiadapiform cf. *Purgatorius* (UCMP 197509, 197517; C), micromomyid plesiadapiform *Dryomomys szalayi* (UM 41870; D), paromomyid plesiadapiform cf. *Ignacius* (USNM 442235, 442240; E), plesiadapid plesiadapiform *Plesiadapis cookei* (UM 87990; F), carpolestid plesiadapiform *Carpolestes simpsoni* (UM 101963; G), adapiform euprimate *Notharctus tenebrosus* (AMNH 11474; H), extant colugo *Cynocephalus volans* (UNSM 15502, AMNH 207001; I), extant arboreal treeshrew *Ptilocercus lowii* (UNSM 488072; J). Right astragali (top three rows) and calcanei (bottom three rows) illustrated in dorsal (top), plantar (middle), and distal (bottom) views. Abbreviations: AEF = astragalar ectal facet; ASF = astragalar sustentacular facet; CEF = calcaneal ectal facet; CF = calcaneocuboid facet; CSF = calcaneal sustentacular facet; LTF = lateral tibial facet; PT = peroneal tubercle. Specimens scaled to proximodistal length. Scale bars for respective astragali (top) and calcanei (bottom) = 1 mm. Some elements reversed to facilitate comparisons. Figure modified from Chester et al. (2015:Fig. S5) and Chester et al. (2017:Fig. 3).

that frequently used orthograde postures on vertical supports and could adjust to an uneven arboreal substrate during locomotion, but with no capacity for specialized running or leaping.

Aspects of the anterior dentition of *T. wilsoni* described here provide additional evidence that this taxon is similar to other plesiolestine palaechthonids such as *P. problematicus* and *P. nacimenti*. The flattened, broad, and dorsomedially oriented lower central incisor morphology of *T. wilsoni* is similar to that of *P. problematicus* and differs from the more laterally compressed ‘semilanceolate’ condition of the palaechthonine *Pa. minor*. The anterior lower tooth crowns preserved in NMMNH P-71598 and NMMNH P-54500 also clearly show that *T. wilsoni* had a large lower canine and smaller second lower premolar, like that of other plesiolestines (Gunnell, 1989; Silcox and Williamson, 2012). Although dental similarities suggest that the plesiolestines *T. wilsoni* and *P. nacimenti* are closely related, evidence for arboreality of *T. wilsoni* does not directly refute the hypothesis that *P. nacimenti* was terrestrial. However, based on evidence for arboreality in *T. wilsoni* and other plesiadapiforms (including the oldest known genus, *Purgatorius*) and on our understanding of positional behaviors and evolutionary relationships among euarchoontan mammals, it seems very likely that plesiadapiforms and other euarchoontans were primitively arboreal (Szalay and Drawhorn, 1980; Bloch and Boyer, 2007; Bloch et al., 2007;

Chester et al., 2015). Therefore, if *P. nacimenti* or any other taxon nested within Euarchonta exhibits terrestrial features, they would be secondarily derived like in the tupaiid treeshrews (Sargis, 2002a,b).

All known partial skeletons of plesiadapiforms are generally similar in possessing many postcranial features related to arboreality, but the various plesiadapiform families exhibit different postcranial features related to differences in their inferred positional behaviors (Bloch and Boyer, 2007). Postcranial comparisons between Palaechthonidae and other plesiadapiform families are currently somewhat limited due to the unknown skeletal elements of *T. wilsoni* (e.g., vertebrae, distal phalanges). Furthermore, the incomplete nature of the postcrania that have been recovered for *T. wilsoni* (NMMNH P-54500) does not allow comparisons of most limb and other body proportions. For example, the carpolestid *Ca. simpsoni* has postcranial specializations for powerfully grasping small diameter branches, including a divergent, opposable hallux with a nail (Bloch and Boyer, 2002), and the presence of these hallux features cannot currently be assessed for *Torrejonia*. However, it seems unlikely that these hallux features were present in palaechthonids because where comparisons can be made, *T. wilsoni* does not have the other specialized features of *Ca. simpsoni*, such as a relatively wider medial epicondyle on the humerus

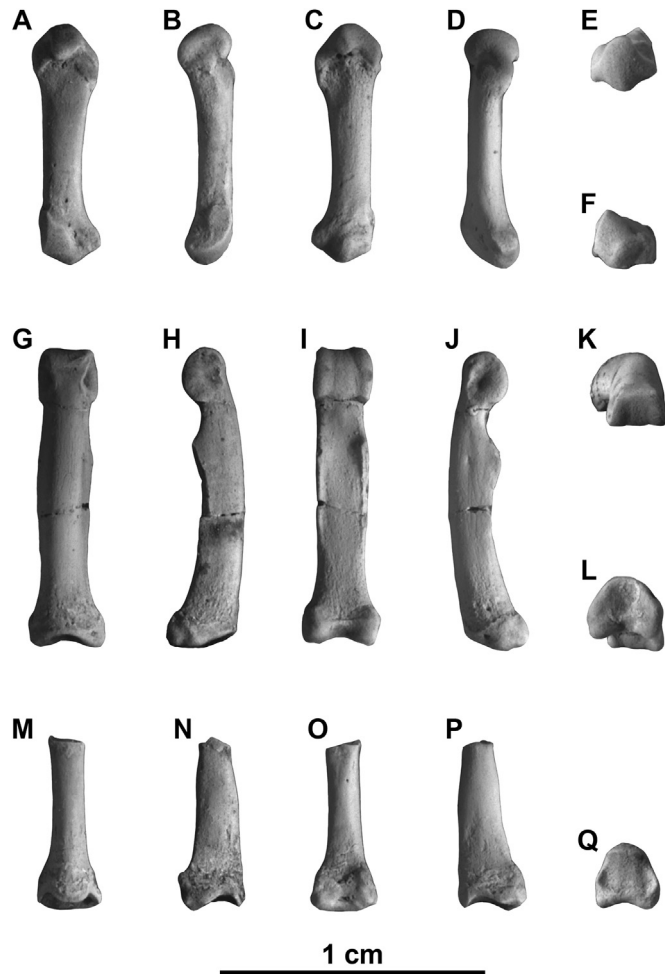


Figure 15. *Torrejonia wilsoni* (NMMNH P-54500) metacarpal and phalanges. A–F) Right fifth metacarpal in dorsal (A), medial (B), palmar (C), lateral (D), distal (E), and proximal (F) views. G–L) Proximal pedal phalanx in dorsal (G), ?medial (H), plantar (I), ?lateral (J), distal (K), and proximal (L) views. M–Q) Proximal half of intermediate phalanx in dorsal (M), ?medial (N), plantar (O), ?lateral (P), and proximal (Q) views.

for enhanced manual grasping, the lack of distinct trochlear ridges on the astragalus for increased mobility at the upper ankle joint (Bloch and Boyer, 2007), or a relatively distally elongate calcaneus potentially related to hallucal grasping (Boyer et al., 2013b; Fig. 14).

The postcranial elements that can be compared across several plesiadapid families are mostly limited to elements that most commonly preserve in the fossil record such as the proximal tarsals. The proximal tarsals of *Torrejonia* are similar to those of the paromomyid *Ignacius* among eucarchontans, but retain some primitive conditions. The astragalar flexor fibularis groove of *T. wilsoni* is not as large and wide as that of micromomyids or those attributed to *Purgatorius* (Chester et al., 2015), and is more like the narrower and likely more derived condition exhibited by paromomyids such as *I. clarkforkensis*. However, the astragalar body of *T. wilsoni* has a defined medial trochlear crest like the astragali of micromomyids and those attributed to *Purgatorius*, whereas this crest is not as defined on the more medially sloping and likely more derived lateral tibial facet of certain paromomyids and plesiadapids (Chester et al., 2015). Other proposed primitive postcranial features documented in *T. wilsoni* include the more distally positioned peroneal process and the more obliquely angled cuboid facet on the calcaneus, which has been hypothesized as the primitive condition among eutherian mammals such as *Protungulatum* (Szalay and Decker, 1974). If correct, these calcaneal features are retentions in

T. wilsoni and are even more primitive than the condition of *Purgatorius*. However, like that of *Purgatorius* and other plesiadapiforms, *T. wilsoni* has derived features compared to *Protungulatum* for more mobility, such as the more concave cuboid facet at the transverse tarsal joint. Overall, these observations suggest that palaechthonids have proximal tarsals that are similar to those of paromomyids, but retain more plesiomorphic features, which has also been suggested for aspects of the cranium and dentition (e.g., Kay and Cartmill, 1977; Silcox et al., 2017).

The remainder of the postcranium of *T. wilsoni* appears to be most similar overall to that of paromomyid plesiadapiforms such as the partial skeletons of latest Paleocene *I. clarkforkensis* (Bloch et al., 2007) and isolated elements attributed to early Eocene *Ph. simonsi* (Beard, 1989, 1993). The striking similarity of certain postcranial elements (e.g., humeri) of *T. wilsoni* and paromomyids may relate to a close phylogenetic relationship, which would be congruent with craniodental evidence supporting these families as closely related among plesiadapiforms within the superfamily Paromomyoidea (Silcox et al., 2017). In fact, the only cladistic analysis to date that incorporates data from the skeleton of *T. wilsoni* supports Palaechthonidae as paraphyletic with *T. wilsoni* as most closely related to Paromomyidae (Chester et al., 2017). Paromomyids have been reconstructed as capable of more frequent pronograde bounding on horizontal branches than other plesiadapiforms, in part based on their limb and trunk proportions, as well as characteristics of their vertebrae, sacrum, and innominate (Bloch et al., 2007; Bloch and Boyer, 2007). Additional postcrania of *T. wilsoni* or other palaechthonid species are needed to assess whether palaechthonids shared some of these features, or whether their postcranial skeleton generally lacks specialized features that characterize other families, as has been noted for the plesiomorphic nature of palaechthonid dentitions (Silcox et al., 2017).

It is also worth considering whether some of the postcranial similarities between *T. wilsoni* and paromomyids might be due to their similar body sizes and whether certain postcranial differences among *T. wilsoni*, the diminutive micromomyids, and some larger-bodied plesiadapids might reflect allometric effects. *Torrejonia wilsoni* is one of the largest palaechthonids (741 g according to the 'All-primate' equation of Conroy, 1987) and has been reconstructed as more frugivorous (Kay and Cartmill, 1977) than several palaechthonids that weighed less than 100 g and were likely more insectivorous (Conroy, 1987; Silcox et al., 2017). Therefore, it would not be surprising if *T. wilsoni* captures only some of the variation in palaechthonid postcranial morphology and positional behaviors, which presumably covary along with a range of different body sizes and diets.

5. Conclusions

The specimens described here provide new information on the skeletal morphology of *T. wilsoni* and insight into the postcranial skeleton and positional behaviors of palaechthonid plesiadapiforms. The most complete dentary of *T. wilsoni* (NMMNH P-71598) preserves previously unknown aspects of the anterior dentition that confirm this species has features similar to other plesiolestine palaechthonids (in contrast to palaechthonines) such as a lanceolate and dorsomedially oriented I_1 and a canine that is considerably larger than P_2 . Postcranial evidence (NMMNH P-54500) suggests that *T. wilsoni* was a committed arborealist capable of clinging and climbing on vertical supports and grasping small diameter branches, like other plesiadapiforms for which postcrania are known. Some postcranial similarities between *T. wilsoni* and paromomyids such as *I. clarkforkensis* and cf. *Ph. simonsi* are rather striking and suggest a close phylogenetic relationship with paromomyids. This is congruent with craniodental evidence supporting Palaechthonidae and Paromomyidae as closely related within the superfamily Paromomyoidea.

Evidence from the proximal tarsals of *T. wilsoni* suggests that palaechthonids retain more plesiomorphic features of the postcranium than paromomyids, which has also been suggested for aspects of the cranium and dentition (e.g., [Kay and Cartmill, 1977](#); [Silcox et al., 2017](#)). In fact, certain features such as a more distally positioned peroneal process on the calcaneus and the oblique orientation of the calcaneocuboid joint may be more plesiomorphic than the condition exhibited by all other known plesiadapiforms including *Purgatorius*. Future discoveries of other palaechthonid postcrania may help elucidate whether *T. wilsoni* adequately characterizes the postcranial morphology of the Palaechthonidae. Such discoveries may also clarify whether palaechthonid postcrania generally lack specialized features that diagnose other plesiadapiform families, as has been suggested for their plesiomorphic dental morphology. Our understanding of euarctontan evolutionary history during the first few million years following the Cretaceous–Paleogene extinction event is still based almost entirely on dentitions of the geologically oldest known plesiadapiforms. Additional discoveries like the skeleton of *T. wilsoni* are needed to document the postcranial and locomotor evolution of stem primates during this critical interval of ecomorphological diversification among placental mammals.

Acknowledgments

We thank Chris Hughes, Shirley Libed, Paul Sealey, Warren Slade, and Ryan and Taylor Williamson for fieldwork, and Pat Hester of the Bureau of Land Management for permits. For access to comparative specimens, we thank the following people and institutions: John Flynn, Division of Vertebrate Paleontology, and Eileen Westwig, Division of Vertebrate Zoology, American Museum of Natural History, New York; William Clemens and Patricia Holroyd, University of California Museum of Paleontology, Berkeley; Larry Heaney and William Stanley, Department of Zoology, Field Museum of Natural History, Chicago; Judy Chupasko, Mammalogy Department, Museum of Comparative Zoology at Harvard University, Cambridge; Philip Gingerich and Gregg Gunnell, University of Michigan Museum of Paleontology, Ann Arbor; Linda Gordon, Kristopher Helgen, Darrin Lunde, and Richard Thorington, Division of Mammals, and Michael Brett-Surman, Department of Paleobiology, United States National Museum of Natural History, Washington, D.C. We thank Doug Boyer (Duke University) and Scott Williams (New York University) for helpful discussions, and Marilyn Fox (Yale Peabody Museum) for preparing, molding, and casting specimens. We thank Joshua Van Houten (Department of Internal Medicine, Yale University) and Morgan Hill and Andrew Smith (Microscopy and Imaging Facility, American Museum of Natural History) for assistance with µCT scanning, and Henry Ermer (Brooklyn College) for help postprocessing µCT scans. We also thank David Alba, an anonymous Associate Editor, and three anonymous reviewers for comments that improved this manuscript. This research was supported by National Science Foundation: NSF EAR-0207750 and 1325544, and DEB 1654952 to T.E.W.; NSF EF-0629836, to J.I.B., M.T.S., and E.J.S.; NSF SBE-1028505 to E.J.S. and S.G.B.C. Additional support was provided by the Leakey Foundation, a Brooklyn College Tow Faculty Travel Fellowship, and a PSC CUNY Award, jointly funded by The Professional Staff Congress and The City University of New York to S.G.B.C., awards from the Bureau of Land Management to T.E.W., and an NSERC Discovery Grant to M.T.S.

References

Argot, C., 2001. Functional-adaptive anatomy of the forelimb in the Didelphidae, and the paleobiology of the Paleocene marsupials *Mayulestes ferox* and *Pucadelphys andinus*. *Journal of Morphology* 247, 51–79.

Beard, K.C., 1989. Postcranial anatomy, locomotor adaptations, and paleoecology of Early Cenozoic Plesiadapidae, Paromomyidae, and Micromomyidae (Eutheria, Dermoptera). Ph.D. Dissertation, Johns Hopkins University School of Medicine.

Beard, K.C., 1991. Vertical postures and climbing in the morphotype of Primatomorpha: implications for locomotor evolution in primate history. In: Coppens, Y., Senut, B. (Eds.), *Origine(s) de la Bipédie Chez les Hominidés*. Éditions du CNRS, Paris, pp. 79–87.

Beard, K.C., 1993. Phylogenetic systematics of the Primatomorpha, with special reference to Dermoptera. In: Szalay, F.S., McKenna, M.C., Novacek, M.J. (Eds.), *Mammal Phylogeny: Placentals*. Springer-Verlag, New York, pp. 129–150.

Bloch, J.I., Boyer, D.M., 2002. Grasping primate origins. *Science* 298, 1606–1610.

Bloch, J.I., Boyer, D.M., 2007. New skeletons of Paleocene-Eocene Plesiadapiformes: a diversity of arboreal positional behaviors in early primates. In: Ravosa, M.J., Dagosto, M. (Eds.), *Primate Origins: Adaptations and Evolution*. Plenum Press, New York, pp. 535–581.

Bloch, J.I., Gingerich, P.D., 1998. *Carpolestes simpsoni*, new species (Mammalia, Proprimates) from the late Paleocene of the Clarks Fork Basin, Wyoming. *Contributions from the University of Michigan Museum of Paleontology* 30, 131–162.

Bloch, J.I., Silcox, M.T., Boyer, D.M., Sargis, E.J., 2007. New Paleocene skeletons and the relationship of “plesiadapiforms” to crown-clade primates. *Proceedings of the National Academy of Sciences of the USA* 104, 1159–1164.

Bloch, J.I., Chester, S.G.B., Silcox, M.T., 2016. Cranial anatomy of Paleogene Micromomyidae and implications for early primate evolution. *Journal of Human Evolution* 96, 58–81.

Brown, T.M., Gingerich, P.D., 1973. The Paleocene primate *Plesiolestes* and the origin of Microsyopidae. *Folia Primatologica* 19, 1–8.

Boyer, D.M., 2009. New cranial and postcranial remains of late Paleocene Plesiadapidae (“Plesiadapiforms,” Mammalia) from North America and Europe: Description and evolutionary implications. Ph.D. Dissertation, Stony Brook University.

Boyer, D.M., Bloch, J.I., 2008. Evaluating the mitten-gliding hypothesis for Paromomyidae and Micromomyidae (Mammalia, “Plesiadapiformes”) using comparative functional morphology of new Paleogene skeletons. In: Sargis, E.J., Dagosto, M. (Eds.), *Mammalian Evolutionary Morphology: A Tribute to Frederick S. Szalay*. Springer, Dordrecht, pp. 233–284.

Boyer, D.M., Prasad, G.V.R., Krause, D.W., Godinot, M., Goswami, A., Verma, O., Flynn, J.J., 2010. New postcrania of *Deccanolestes* from the Late Cretaceous of India and their bearing on the evolutionary and biogeographic history of euarctontan mammals. *Naturwissenschaften* 97, 365–377.

Boyer, D.M., Yapuncich, G.S., Chester, S.G.B., Bloch, J.I., Godinot, M., 2013a. Hands of early primates. *Yearbook of Physical Anthropology* 57, 33–78.

Boyer, D.M., Seiffert, E.R., Gladman, J.T., Bloch, J.I., 2013b. Evolution and allometry of calcaneal elongation in living and extinct primates. *PLoS One* 8, e67792.

Boyer, D.M., Yapuncich, G.S., Chester, S.G.B., Bloch, J.I., Godinot, M., 2016. Hands of Paleogene primates. In: Kivell, T.L., Lemelin, P., Richmond, B.G., Schmitt, D. (Eds.), *The Evolution of the Primate Hand: Anatomical, Developmental, Functional, and Paleontological Evidence*. Springer Publishing, New York, pp. 373–419.

Chester, S.G.B., Bloch, J.I., 2013. Systematics of Paleogene Micromomyidae (Euarctonta, Primates) from North America. *Journal of Human Evolution* 65, 109–142.

Chester, S.G.B., Sargis, E.J., Szalay, F.S., Archibald, J.D., Averianov, A.O., 2010. Mammalian distal humeri from the Late Cretaceous of Uzbekistan. *Acta Palaeontologica Polonica* 55, 199–211.

Chester, S.G.B., Sargis, E.J., Szalay, F.S., Archibald, J.D., Averianov, A.O., 2012. Therian femora from the Late Cretaceous of Uzbekistan. *Acta Palaeontologica Polonica* 57, 53–64.

Chester, S.G.B., Bloch, J.I., Boyer, D.M., Clemens, W.A., 2015. Oldest known euarctontan postcrania and affinities of Paleocene *Purgatorius* to Primates. *Proceedings of the National Academy of Sciences of the USA* 112, 1487–1492.

Chester, S.G.B., Williamson, T.E., Bloch, J.I., Silcox, M.T., Sargis, E.J., 2017. Oldest skeleton of a plesiadapiform provides additional evidence for an exclusively arboreal radiation of stem primates in the Paleocene. *Royal Society Open Science* 4, 170329.

Conroy, G.C., 1987. Problems of body-weight estimation in fossil primates. *International Journal of Primatology* 8, 115–137.

Gebo, D.L., Sargis, E.J., 1994. Terrestrial adaptations in the postcranial skeletons of guenons. *American Journal of Physical Anthropology* 93, 341–371.

Gebo, D.L., Smith, R., Dagosto, M., Smith, T., 2015. Additional postcranial elements of *Teilhardina belgica*: the oldest European primate. *American Journal of Physical Anthropology* 156, 388–406.

Gingerich, P.D., Gunnell, G.F., 2005. Brain of *Plesiadapis cookei* (Mammalia, Proprimates): surface morphology and encephalization compared to those of Primates and Dermoptera. *Contributions from the Museum of Paleontology*, The University of Michigan 31, 185–195.

Godinot, M., Beard, K.C., 1991. Fossil primate hands: a review and an evolutionary inquiry emphasizing early forms. *Human Evolution* 6, 307–354.

Gunnell, G.F., 1989. Evolutionary history of Microsyopidae (Mammalia, ?Primates) and the relationship between plesiadapiforms and primates. *University of Michigan Papers on Paleontology* 27, 1–157.

Kay, R.F., Cartmill, M., 1974. Skull of *Palaechthon nacimenti*. *Nature* 252, 37–38.

Kay, R.F., Cartmill, M., 1977. Cranial morphology and adaptations of *Palaechthon nacimenti* and other Paromomyidae (Plesiadapoidea, ?Primates), with a description of a new genus and species. *Journal of Human Evolution* 6, 19–53.

Ksepka, D.T., Stidham, T.A., Williamson, T.E., 2017. Early Paleocene landbird supports rapid phylogenetic and morphological diversification of crown birds after K-Pg mass extinction. *Proceedings of the National Academy of Sciences of the USA* 114, 8047–8052.

Leslie, C.E., Peppe, D.J., Williamson, T.E., Bilardello, D., Heizler, M., Secord, R., Leggett, T., 2018. High-resolution magnetostratigraphy of the Upper Nacimiento Formation, San Juan Basin, New Mexico, USA: implications for basin evolution and mammalian turnover. *American Journal of Science* 318, 300–334.

Loggren, D.L., Lillegraven, J.A., Clemens, W.A., Gingerich, P.D., Williamson, T.E., 2004. Paleocene biochronology; the Puercan through Clarkforkian land mammal ages. In: Woodburne, M.O. (Ed.), *Late Cretaceous and Cenozoic Mammals of North America*. Columbia University Press, New York, pp. 43–105.

Ni, X., Gebo, D.L., Dagosto, M., Meng, J., Tafforeau, P., Flynn, J.J., Beard, K.C., 2013. The oldest known primate skeleton and early haplorhine evolution. *Nature* 498, 60–64.

Ni, X., Li, Q., Li, K., Beard, K.C., 2016. Oligocene primates from China reveal divergence between African and Asian primate evolution. *Science* 352, 673–677.

Ogg, J.G., 2012. Geomagnetic polarity time scale. In: Gradstein, F.M., Ogg, J.G., Schmitz, M.D., Ogg, G. (Eds.), *The Geologic Time Scale 2012*. Elsevier, Oxford, pp. 85–113.

Orliac, M.J., Ladevèze, S., Gingerich, P.D., Lebrun, R., Smith, T., 2014. Endocranial morphology of Paleocene *Plesiadapis tricuspidens* and evolution of the early primate brain. *Proceedings of the Royal Society B* 281, 20132792.

Prasad, G.V.R., Godinot, M., 1994. Eutherian tarsal bones from the Late Cretaceous of India. *Journal of Paleontology* 68, 892–902.

Sargis, E.J., 2001. A preliminary qualitative analysis of the axial skeleton of tupaiids (Mammalia, Scandentia): functional morphology and phylogenetic implications. *Journal of Zoology*, London 253, 473–483.

Sargis, E.J., 2002a. Functional morphology of the forelimb of tupaiids (Mammalia, Scandentia) and its phylogenetic implications. *Journal of Morphology* 253, 10–42.

Sargis, E.J., 2002b. The postcranial morphology of *Ptilocercus lowii* (Scandentia, Tupaiidae): an analysis of primatomorphan and volitantian characters. *Journal of Mammalian Evolution* 9, 137–160.

Sargis, E.J., 2002c. Functional morphology of the hindlimb of tupaiids (Mammalia, Scandentia) and its phylogenetic implications. *Journal of Morphology* 254, 149–185.

Silcox, M.T., 2001. A phylogenetic analysis of Plesiadapiformes and their relationship to Euprimates and other archontans. Ph.D. Dissertation, Johns Hopkins University School of Medicine.

Silcox, M.T., 2008. The biogeographic origins of Primates and Euprimates: east, west, north, or south of Eden? In: Sargis, E.J., Dagosto, M. (Eds.), *Mammalian Evolutionary Morphology: A Tribute to Frederick S. Szalay*. Springer, Dordrecht, pp. 199–231.

Silcox, M.T., Williamson, T.E., 2012. New discoveries of early Paleocene (Torrejonian) primates from the Nacimiento Formation, San Juan Basin, New Mexico. *Journal of Human Evolution* 63, 805–833.

Silcox, M.T., Dalmyn, C.K., Bloch, J.I., 2009. Virtual endocast of *Ignacius graybullianus* (Paromomyidae, Primates) and brain evolution in early primates. *Proceedings of the National Academy of Sciences of the USA* 106, 10987–10992.

Silcox, M.T., Benham, A.E., Bloch, J.I., 2010. Endocasts of *Microsyops* (Microsyopidae, Primates) and the evolution of the brain in primitive primates. *Journal of Human Evolution* 58, 505–521.

Silcox, M.T., Bloch, J.I., Boyer, D.M., Chester, S.G.B., López-Torres, S., 2017. The evolutionary radiation of plesiadapiforms. *Evolutionary Anthropology* 26, 74–94.

Simpson, G.G., 1935. The Tiffany fauna, upper Paleocene. II.— Structure and relationships of *Plesiadapis*. *American Museum Novitates* 816, 1–30.

Szalay, F.S., 1969. Mixodectidae, Microsyopidae, and the insectivore-primate transition. *Bulletin of the American Museum of Natural History* 140, 195–330.

Szalay, F.S., 1981. Phylogeny and the problem of adaptive significance: the case of the earliest primates. *Folia Primatologica* 36, 157–182.

Szalay, F.S., Dagosto, M., 1980. Locomotor adaptations as reflected on the humerus of Paleogene primates. *Folia Primatologica* 34, 1–45.

Szalay, F.S., Decker, R.L., 1974. Origins, evolution, and function of the tarsus in Late Cretaceous Eutheria and Paleocene primates. In: Jenkins F.A. Jr., (Ed.), *Primate Locomotion*. Academic Press, New York, pp. 223–259.

Szalay, F.S., Drawhorn, G., 1980. Evolution and diversification of the Archonta in an arboreal milieu. In: Luckett, W.P. (Ed.), *Comparative Biology and Evolutionary Relationships of Tree Shrews*. Plenum Press, New York, pp. 133–169.

Szalay, F.S., Sargis, E.J., 2001. Model-based analysis of postcranial osteology of marsupials from the Palaeocene of Itaboraí (Brazil) and the phylogenetics and biogeography of Metatheria. *Geodiversitas* 23, 139–302.

Szalay, F.S., Tattersall, I., Decker, R.L., 1975. Phylogenetic relationships of *Plesiadapis* – postcranial evidence. In: Szalay, F.S. (Ed.), *Approaches to Primate Paleobiology*. Karger, Basel, pp. 136–166.

Williamson, T.E., 1996. The beginning of the age of mammals in the San Juan Basin, New Mexico: biostratigraphy and evolution of Paleocene mammals of the Nacimiento Formation. *New Mexico Museum of Natural History and Science Bulletin* 8, 1–141.

Wilson, R.W., Szalay, F.S., 1972. New paromomyid primate from middle Paleocene beds, Kutz Canyon area, San Juan Basin, New Mexico. *American Museum Novitates* 2499, 1–18.

Wood, H.E., Chaney, R.W., Clark, J.M., Colbert, E.H., Jepsen, G.L., Reeside J.R. Jr., Stock, C., 1941. Nomenclature and correlation of the North American continental Tertiary. *Geological Society of America Bulletin* 52, 1–48.